Empirical Market Design in Surplus Food Marketplaces

Alexandra Yizhuo Dong[*]   Auyon Siddiq[†]   Jingwei Zhang[‡]

November 6, 2025

Abstract

Commercial food waste presents a major challenge to urban sustainability. In response, digital platforms have emerged that create new marketplaces for food retailers (e.g. bakeries) to sell surplus inventory at a discount. We consider how a key market design lever – the platform's pricing policy – influences seller entry and food waste diverted (i.e., aggregate sales volume) in a major surplus food marketplace. We estimate a structural model of a two-sided marketplace that captures both spatially differentiated consumer demand and sellers' market entry decisions, using hourly inventory data from 465 participating food retailers across four U.S. urban centers (Manhattan, Boston, San Francisco, and Seattle). Central to our methodology is a new estimation technique for sellers' entry costs grounded in discrete optimization, which dramatically speeds up estimation compared to standard nested fixed-point methods. We find significant heterogeneity across the four cities in consumers' travel costs and sensitivity to sellers' on-platform ratings. Counterfactual results show that seller participation is more price-elastic than consumer demand, implying that supply constraints primarily determine the volume of food waste diverted by the marketplace. Delegating price control to sellers invites excessive competition and induces exit, leading to a sharp contraction in equilibrium sales volume. Overall, our findings support platform control of prices in surplus food marketplaces – provided discounts are not too steep – and offer guidance to platform operators seeking to stimulate seller entry and curb food waste.

Keywords: Food waste, entry games, structural estimation, integer optimization, market design, Too Good to Go.

---

[*]Anderson School of Management, University of California, Los Angeles, `yizhuo.dong.phd@anderson.ucla.edu`.

[†]Anderson School of Management, University of California, Los Angeles, `auyon.siddiq@anderson.ucla.edu`.

[‡]SC Johnson Colleage of Business, Cornell University, `jz2293@cornell.edu`.

1 Introduction

Food waste is a pressing global issue, with approximately one-third of all food produced—around 1.3 billion tons—going to waste each year, and costing as much as $400 billion annually (WRAP, 2015). This waste occurs at every stage of the supply chain, from farms discarding cosmetically imperfect produce to retailers and restaurants disposing of unsold inventory (Akkaş and Gaur, 2022). In the United States, 31% of the food waste occurs at the retail and consumer levels, highlighting a need for better redistribution systems to reduce food waste (U.S. Department of Agriculture, 2025). Beyond the economic costs, food waste contributes to environmental degradation through greenhouse gas emissions and diversion to landfills, undermining the sustainability of urban centers where consumption and waste are most concentrated.

The challenge of reducing urban food waste has been met by the emergence of new two-sided platforms that enable food retailers (e.g., restaurants, bakeries, and coffee shops) to sell excess food in a "surplus market", where consumers can purchase items – usually at a significant discount – that would otherwise be discarded. For instance, on the platform Too Good to Go, bakeries can offer unsold pastries in the surplus market at a fraction (e.g., $\frac{1}{3}$) of their original price; the platforms Food For All, Karma, Olio, and Phenix operate similarly, although with some variation in the precise market designs. The promise of these platforms is that they offer a market-based solution to food waste by creating value for all parties: Retailers can recover costs on inventory that would otherwise have little salvage value, and consumers can access quality food at reduced prices.

Surplus food marketplaces, whose mission is to minimize food waste at scale (Too Good To Go, 2024), have been shown to exhibit indirect network effects (Richards and Hamilton, 2018). This suggests that participation from a broad set of retailers is especially important for these platforms to achieve the sales volume necessary to meaningfully reduce waste.[1] However, the decision to participate is non-trivial for retailers due to a challenging profitability environment – consumers expect steep discounts on surplus food, which puts pressure on prices, and perishability limits retailers' on–hand inventory, further restricting revenue. Additionally, despite sunk production, entering and operating in these marketplaces is not costless for retailers.[2] As a result, making entry sufficiently attractive for food retailers requires careful market design.

A platform's pricing policy is an especially important design lever for surplus food marketplaces. In addition to shaping consumer demand, the platform's adopted discount rate plays a critical role in

---

[1]See Armstrong (2006) for a general discussion of network effects in two-sided markets.

[2]Examples of fixed and marginal costs include platform subscription fees, staff training, packaging, integration into existing point-of-sale and inventory systems, and disruptions to regular store operations.

determining supply-side entry into the marketplace, given the notoriously tight margins in food retail (Restaurant365, 2023). In practice, platforms vary in their pricing policies – for example, Too Good to Go uniformly mandates that food retailers discount items by two-thirds of their retail value, whereas Flashfood grants retailers more flexibility in pricing, although still imposes a minimum discount of 50% (Vachon, 2025).

Further, given potential heterogeneity in retailers' costs, a natural question platforms face is whether to delegate price control to retailers, so to lift their margins and increase the appeal of joining the marketplace. However, the impact of delegating pricing on the marketplace's ability to divert food waste is ambiguous, because the ensuing price competition is likely to shift both consumer demand and retailers' entry decisions in equilibrium. Consequently, determining the net effect of price competition requires carefully accounting for its impact on both sides of the marketplace. Moreover, because urban characteristics may shape consumer demand patterns (e.g., by influencing travel costs), the performance of different pricing mechanisms is likely to vary across geographic markets.

1.1 Contributions

This paper examines the role of a platform's pricing policy and the urban environment in shaping outcomes in a surplus food marketplace. Specifically, given the importance of retailer participation and waste diversion, we ask:

1. *How do consumer preferences in surplus food marketplaces vary across urban environments?*
2. *Do demand- or supply-side effects dominate in response to market-wide price changes?*
3. *How does permitting seller price competition impact seller entry and aggregate sales volume?*

We address these questions by estimating a structural model of a two-sided marketplace where both sellers and consumers are spatially differentiated. The model captures the role of price and urban characteristics in shaping both consumer demand and sellers' strategic entry decisions. We focus on aggregate sales volume as our outcome of interest, which serves as a proxy for the total amount of food waste diverted as a result of transactions in the marketplace.

We estimate our model using a detailed dataset from a major platform that operates surplus food marketplaces internationally, focusing on four U.S. urban centers: Boston, Manhattan, San Francisco, and Seattle. The data comprises hourly observations of sellers' surplus inventory levels, prices, ratings, and other attributes over a 10-week period from March to May 2024, covering 465 participating retailers and about 653,000 observations at the seller-hour level. This temporal and spatial granularity allows us to observe detailed store-level operations—specifically, the depletion and replenishment of inventory—as

well as spatial variation in consumer demand patterns. We supplement this platform data with Google Places information on all food-related establishments (whether participating in the marketplace or not) and US Census (American Community Survey) data on local demographics, which helps us account for urban characteristics that influence demand and entry.

Our model aims to capture both sides of the market: Consumers' food purchase choices and sellers' entry decisions. On the demand side, we model consumer arrivals as varying in space and time. Conditional on arrival, consumers' seller choices follow a multinomial logit (MNL) model that accounts for consumer-seller distances and seller attributes. In estimating the demand model, we instrument for consumer-seller distances to address potential endogeneity in sellers' locations, since sellers' decision to enter the marketplace may depend on local unobserved demand shocks. On the supply-side, we model seller entry as a non-cooperative game where each seller makes a strategic entry decision based on their expected profit in equilibrium, which depends on both consumer demand and the entry decisions of competing sellers.

We contribute to the literature on empirical models of market entry by proposing a new estimation technique that uses integer optimization to recover sellers' cost parameters in the spirit of generalized methods of moments (Hansen, 1982). At a high level, our approach has two steps. First, we use a generic random forest to construct a large pool of "candidate equilibria", which are binary vectors that can be interpreted as plausible solutions to the sellers' entry game. Second, we solve a large-scale integer optimization problem that matches moments by jointly searching over the pool of candidate equilibria and the set of unknown parameters. To investigate its performance, we compare our approach to a straightforward implementation of a nested-fixed point (NFXP) algorithm (Rust, 1987) within a simulated methods of moments (McFadden, 1989) framework. Numerical results show our method dramatically speeds up estimation compared to the NFXP algorithm – in some synthetic instances, by an order of magnitude – which allows our model to scale to a larger number of covariates and capture a richer description of market behavior.

Our estimates reveal substantial heterogeneity in consumers' sensitivity to distance and sellers' ratings across markets. Consumers in San Francisco and Seattle face travel costs of close to $1/km, compared to $0.36/km and $0.48/km in Manhattan and Boston. Cities with lower travel costs see far greater consumer sensitivity to ratings: A one-star increase in a seller's on-platform rating is valued at roughly $4 to $6 in Manhattan and Boston, but less than $2 in San Francisco and Seattle. These results suggests that food retailers in commercially dense and accessible urban centers face more competitive pressure to maintain strong on-platform reputations, and consequently the impact of the platform's pricing policy may vary substantially across markets.

We use our estimates to address two counterfactuals. First, we consider *uniform pricing*, where the platform mandates a common discount rate throughout the market, and vary the discount rate from 0 to 100%. We find that the supply response (i.e., changes in seller entry) dominates the effect on consumer demand for a wide range of prices; in most markets, supply is more elastic for all discount rates above 25-30%. This suggests that the total food waste diverted by the marketplace is dictated primarily by seller participation, and that deep discounts on surplus food may be highly sub-optimal. In the second counterfactual, we consider *delegated pricing*, where sellers to engage in Bertrand-Nash price competition, rather than adhering to a platform-specified uniform discount. Under delegated pricing, sales volumes contract sharply in all markets, potentially by up to $58 - 83\%$, suggesting that permitting individual sellers to set prices can harm the marketplace by inviting excessive competition, eroding profit margins and driving sellers to exit.[3]

Overall, our findings provide guidance to designers of surplus food marketplaces seeking to stimulate seller participation and increase the volume of food waste diverted. Our results provide support for platforms maintaining control over market prices – which relieves sellers of competitive pressure – but warns against mandating excessively steep discounts due to the harms to seller profitability. More broadly, the results illustrate that a platform's choice of pricing policy is central to the effective design of surplus food marketplaces.

The remainder of the paper is organized as follows. Section 2 provides an overview of the marketplace and the data. Section 3 develops our two-sided structural model of consumer demand and seller entry decisions. Section 4 discusses demand estimation, including the instrument for consumer–seller distances. Section 5 presents our discrete optimization method for estimating sellers' cost parameters. Section 6 reports parameter estimates and model fit, and Section 7 presents the two counterfactual analyses. Section 8 concludes.

1.2 Related Literature

This paper contributes to the literature on empirical models of market entry, demand estimation with spatially differentiated products, and market-based solutions for reducing food waste.

Empirical models of market entry. Foundational work on market entry includes Bresnahan and Reiss (1991), Berry (1992), Mazzeo (2002), and Seim (2006). We refer the reader to Berry and Reiss (2007) for a review of seminal work on estimating entry models and Aguirregabiria and Suzuki (2016) for a review of entry under spatial competition.

---

[3]Our findings align with the theoretical analysis in (Cachon et al., 2025), who provide conditions under which decentralized pricing can harm platform profits, as a consequence of competition suppressing sellers' prices.

We contribute to the operations management literature that estimates a structural model of market entry. For example, Wang et al. (2023) investigate entry of generic drug manufacturers. Following Berry (1992), they model each firm's profit as a linear function of the number of competitors, whereas we allow entry to modify consumers' choice sets within a logit-based demand model, similar to Lee and Musolff (2023).

In general, estimating entry models is computationally challenging because players' decisions are binary (i.e., to enter or not), and payoffs depend on the binary decisions of other players, leading to fixed-point equilibrium conditions with discrete variables that must be enforced within the estimator (Bajari et al., 2007). Prior work has addressed these challenges by adopting a policy function approach, which treats entry decisions as reduced-form functions of observables (Jia, 2008; Collard-Wexler, 2013). A limitation of policy functions is that they approximate rather than explicitly model equilibrium behavior. A more precise alternative is to explicitly enforce the equilibrium and optimize over the parameter space through a nested fixed-point (NFXP) algorithm (Ciliberto and Tamer, 2009; Ciliberto et al., 2021; Lee and Musolff, 2023). However, NFXP methods are known to be extremely computationally expensive due to the need to re-solve for the equilibrium at each candidate parameter vector (Su and Judd, 2012), and can become intractable for even moderately sized parameter spaces.

To overcome the computational challenges of NFXP methods, we develop a new estimation technique for entry models using the paradigm of integer optimization (Wolsey, 2020). Like NFXP, our approach enforces equilibrium conditions exactly, but eliminates the need to iteratively re-solve for the equilibrium by directly embedding the relevant equilibrium conditions into the optimization model. This formulation allows for a more scalable estimation process and enables the incorporation of additional covariates that would be nonviable under traditional NFXP.

Demand estimation with spatially differentiated products. Our demand model follows the celebrated discrete choice literature for differentiated products (Berry et al., 1995; Nevo, 2001). To account for heterogeneity in consumer preferences over product locations, Davis (2006) and Thomadsen (2007) incorporate geographic distance into consumer utility. Spatial demand models have also been used in the context of urban mobility (Kabra et al., 2020; He et al., 2021; Stourm and Stourm, 2024; Liu et al., 2024) and public health (Bravo et al., 2024). While these papers differ in application, they share with our work a focus on how the spatial distribution of products influence consumer demand.

We extend the literature on spatial demand models by addressing endogeneity in consumer-seller distances, since seller entry may be influenced by unobserved local market conditions. To our knowledge, the only other study to consider endogeneity in consumer-seller distance is Cao et al. (2024), who construct instruments based on the income distribution within fixed radii from the city center. In

contrast, we instrument for distance using historical landmarks (i.e., city halls and courthouses), whose locations are plausibly tied to the emergence of long-standing commercial districts (for example, due to historical land use patterns) but are unlikely to be correlated with modern consumer preferences or platform-specific demand shocks. In addition to addressing distance endogeneity, we extend the literature on spatial demand models by integrating our demand estimates into a supply-side model of seller profit and entry, allowing us to investigate how geographic variation in demand shapes market structure in urban settings.

Market-based solutions for reducing food waste. Food waste arises at every stage of the supply chain, motivating a rich literature on questions related to incentives, coordination, and innovative business models for waste mitigation (Akkaş and Gaur, 2022). Considerable prior work has focused on operational aspects of food waste reduction in primary markets, including restaurants (Astashkina et al., 2024), commercial kitchens (Yu et al., 2023), and grocery retail (Belavina et al., 2017; Astashkina et al., 2019; Belavina, 2021; Park et al., 2022; den Boer et al., 2022; Jain et al., 2023; Sanders, 2024; Zhou et al., 2024a; Kazaz et al., 2025).

Our work contributes to an emerging literature that examines how new marketplaces can reduce waste by more efficiently re-allocating surplus food that would otherwise be discarded (Richards and Hamilton, 2018; Makov et al., 2020; Manshadi and Rodilitz, 2020; de Almeida Oroski and da Silva, 2023; Alptekinoglu and Benade, 2024). Within this stream, Yang and Yu (2025) analyze the platform Too Good to Go and compare the performance of various clearance policies with respect to waste reduction and store profit. Zhou et al. (2024b) study the same platform, focusing on the optimal bundling of surplus inventory into discrete units for sale ("surprise bags"). Our paper complements this work by empirically investigating how the platform's policies regarding pricing and competition shape seller participation and waste diversion.

More broadly, our work contributes to a growing literature that uses empirical methods to study the operations of digital platforms, with contextual areas including delivery and urban mobility (Lu et al., 2023; Zhang et al., 2023; Cui et al., 2024; Clyde et al., 2024; Guo et al., 2025), labor marketplaces (Cao et al., 2022; Besbes et al., 2023), home-sharing (Cui et al., 2020a), social media (Zeng et al., 2023, 2024; Hu et al., 2024), and online retail (Cui et al., 2019; Zhang et al., 2019; Cui et al., 2020b; Bai et al., 2022a,b; Calvo et al., 2023; Long et al., 2024; Jiang et al., 2025).

2 Data and Marketplace Overview

Our study focuses on four urban centers in the U.S.: Boston, Manhattan, San Francisco, and Seattle. For each of these markets, we obtained data from three sources: (1) Too Good To Go, a digital platform that operates surplus food marketplaces, (2) the Google Places API (Google Maps Platform, 2025), which provides information on the commercial environment, and (3) the American Community Survey (U.S. Census Bureau, 2022), which provides demographic data. We provide an overview of each of these datasets next, focusing on the platform.

2.1 Platform Data

To Good to Go is a major two-sided marketplace for connecting food retailers with consumers to reduce food waste. The platform claims to be the world's largest marketplace for surplus food with a total of 100 million users (Too Good To Go, 2024). Each day, participating retailers (such as bakeries, cafes and restaurants) package unsold inventory into "bags", which are listed and sold at a significantly lower price – currently $\frac{1}{3}$ of the bag's retail value in our focal markets. Consumers can reserve and purchase bags directly through the platform's app, and must travel to the store to pick up their purchase in-person. Prior to making a purchase, consumers can view several store features, including the store's rating, distance, pickup time window, bag price, and the number of bags available. Figure 11 in the Appendix shows an example of a consumer's view of the app.

The dataset comprises hourly, store-level observations from each of the four cities collected over a 64-day period from March 1 to May 13 in 2024.[4] Bags sold on the platform are grouped into four categories: Meals, Baked Goods, Groceries, and Other. Our analysis focuses on the largest category, Baked Goods, which accounts for 38% of all stores. In total, the dataset contains 653,000 observations from 465 stores. Summary statistics are presented in Table 1.

Table 1: Summary Statistics (Baked Good Category).

	Manhattan	San Francisco	Boston	Seattle	Total
Number of Bakeries	284	94	34	53	465
Number of Observations	418,473	128,623	52,719	53,484	653,299
Quantity Sold (Bags)	34,827	6,243	2,896	2,575	46,541
Revenue ($)	188,189	31,658	14,882	14,809	249,539

Each observation contains information on the store's name, product category, geographic location (i.e., lat/long coordinates), pickup time, retail value, price, current inventory level, store ratings, and the stock-out time (if any). Table 8 in Appendix A shows an example of three observations from a

---

[4]We collected data over this time period for Manhattan, San Francisco, and Boston. For Seattle, the data spans a 45-day period within this time period.

three-hour window for a single store selling baked goods. We briefly comment on the key variables next.

Inventory. Store inventory is measured by the number of bags listed on the platform – Figure 1 depicts the depletion and replenishment of inventory for two example stores. Because inventory fluctuates hourly, customers arriving to the app at different points in time may see different options, motivating us to model consumers' choice sets as being dynamic. Stock-outs are frequent, with stores lacking inventory in 63% of observations. Higher-rated stores are stocked-out more frequently: Those above the median rating in the market have no inventory in 82% of observations, compared to 76% for those below the median. Figure 1 shows two Manhattan bakeries with similar daily inventory but notable differences in depletion rates. This highlights heterogeneity among sellers: Some stores face chronic excess demand, while other stores are unable to clear their inventory, creating inefficiencies that limit the platform's ability to reduce food waste.

Figure 1: Example of Inventory Cycles For Two Stores in Manhattan.

Store A (Rating: 4.6/5.0).

Store B (Rating: 4.0/5.0).

Retail value and price. On the platform, stores report the retail value of a bag, and the selling price is automatically set to $\frac{1}{3}$ of that value, which typically does not change from day to day.[5] We refer to the ratio between the platform price and retail value as the *price ratio*. The left panel of Figure 2 shows a weak correlation between price and sale probability, suggesting the presence of confounding factors, which may include consumers' travel costs and store ratings.

---

[5]Over our 10-week observation period, only 0.8% of bakeries across the four cities had at least one change of price.

Sellers' on-platform ratings. Empirically, we observe a strong positive correlation between a store's rating on the platform and the probability of a sale in any given hour (right panel of Figure 2), consistent with prior literature documenting positive associations between customer ratings and sales performance (Chevalier and Mayzlin, 2006; Anderson and Magruder, 2012).

Figure 2: Sales Probability vs. Price and Ratings in Manhattan.
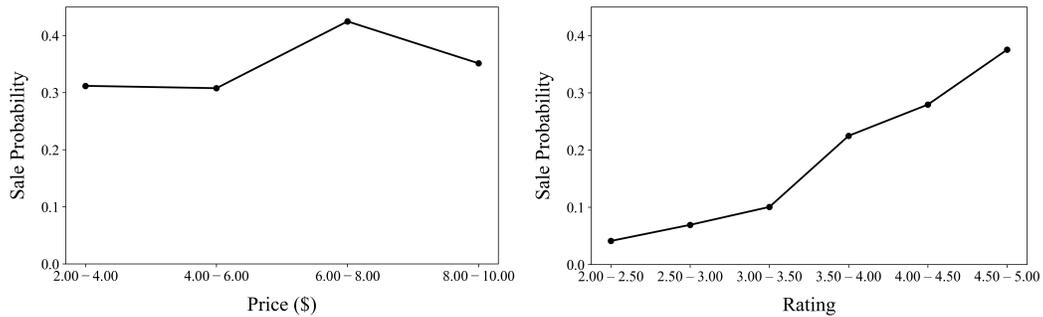
Notes: The vertical axis represents the average probability that a store makes a sale in a given hour, binned by seller price and rating.

Location and distance. Although purchases occur on a digital platform, customers must collect their items in-person, making travel costs a potentially important driver of consumer demand. The platform's default search radius reinforces this (Figure 11). In Manhattan, for instance, sales generally correlate with population density (Figure 3), with strong demand in dense areas like the Upper East Side. These patterns motivate incorporating population density and consumer–seller distances into the demand model, using census tract fixed effects and instrumental variables to address endogeneity.

10

Figure 3: Average Daily Sales and Population Density in Manhattan.
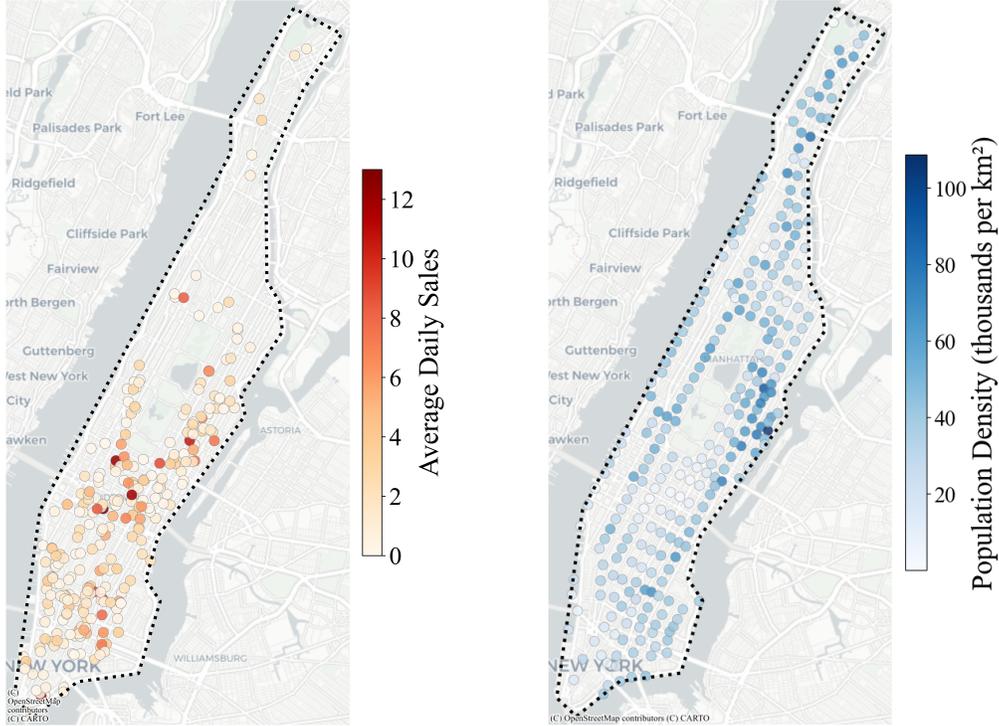
Average daily sales by store.   Population density by census tract.

2.2 Commercial and Demographic Data

We used the Google Places API (Google Maps Platform, 2025) to collect data in March 2024 across the four markets, which covers all relevant stores listed on Google Maps, including both participants and non-participants on the platform. Within the Google API, we extract all establishments that have the assigned place type of "bakery" or "coffee shop". Each observation contains store attributes such as geographic location, Google rating, operating hours, and a brief text description of the store. This data is primarily used to estimate the cost functions underlying stores' entry decisions (see Section 5). We also draw on the 2022 American Community Survey (ACS) 5-Year Estimates (U.S. Census Bureau, 2022), a comprehensive dataset produced by the U.S. Census Bureau that provides demographic and socio-economic information at the census tract level. In particular, we use data on household income and population density to capture spatial heterogeneity in consumer demand (see Section 3.1). Appendix B presents descriptive statistics for the Google Places and ACS variables.

3 Model

This section presents our structural model of the two-sided marketplace. Section 3.1 develops the model for consumer demand, defined by both consumers' arrivals and choices. Section 3.2 develops the

supply-side model of sellers' costs and market entry decisions. Section 3.3 discusses market equilibrium and outlines the key assumptions that make estimation tractable. The model described below is for a single market, we estimate it separately for each of the four markets in our sample.

3.1 Consumer Arrivals and Choice

On the demand-side, we model consumer behavior in two stages. The first is an *arrival* model, which captures the base market size – specifically, the number of consumers at a given location intending to make a purchase. The second component is a *choice* model, which characterizes the probability that each of these consumers purchases a bag from each seller.[6] The model explicitly accounts for both temporal and spatial heterogeneity in demand. Time is indexed by the pair $(t, \tau) \in \mathcal{T} \times \mathcal{T}$, where t denotes a granular time period (e.g., hour of the day) and τ represents a higher-level time period (e.g., day of the month). This distinction allows us to capture temporal variation in market conditions at different levels of aggregation. Consumers are spatially heterogeneous and distributed over a finite number of locations, indexed by the set $\mathcal{L}$. The consumer population arriving at location $\ell \in \mathcal{L}$ during market (t, τ) is then given by

$$\lambda_{\ell\tau}^t(\boldsymbol{\alpha}) = \alpha_0 + \boldsymbol{\alpha}^\top \mathbf{y}_{\ell\tau}^t,$$

where $\mathbf{y}_{\ell\tau}^t$ is a vector of location- and time-specific covariates (e.g., population density, time of day indicators) and $\boldsymbol{\alpha}$ is the corresponding parameter vector.

Consumers' choice sets are shaped by sellers' entry decisions. Let $\mathcal{J}$ denote the set of all possible sellers. Let $\boldsymbol{\psi} \subset \{0,1\}^{|\mathcal{J}|}$ denote the strategy profile of all sellers, where $\psi_j = 1$ if seller j enters and $\psi_j = 0$ otherwise. Let $\mathcal{J}^+(\boldsymbol{\psi}) = \{j \in \mathcal{J} : \psi_j = 1\}$ be the set of stores that enter the market. The deterministic component of consumer utility for seller in the market $j \in \mathcal{J}^+$ for consumers at location ℓ is then given by

$$V_{j\ell}(\boldsymbol{\beta}) = \beta_0 + \boldsymbol{\beta}^\top \mathbf{x}_{j\ell} + \delta_\ell + \xi_j,$$

where $\mathbf{x}_{j\ell}$ is a vector of seller- and consumer-specific covariates (such as store ratings, distance between consumer and store, and price) and $\boldsymbol{\beta}$ parameterizes preferences over these attributes. The fixed-effect δ_ℓ captures consumer-location characteristics and ξ_j denotes the unobserved component of utility for seller j. Consumers arriving at different points in time may face different choice sets due to inventory stock-outs. Let $\mathcal{J}_\tau^t(\boldsymbol{\psi}) \subseteq \mathcal{J}^+(\boldsymbol{\psi})$ denote the set of sellers that have both entered the market and have available inventory at time (t, τ).

A consumer's total utility is given by $V_{j\ell}(\boldsymbol{\beta}) + \epsilon_{j\ell}^t$, where the $\epsilon_{j\ell}^t$ terms are idiosyncratic shocks and

---

[6] Each consumer is assumed to purchase at most one bag per transaction, and multiple-bag purchases are treated as independent transactions.

assumed to be i.i.d. draws from the Gumbel distribution, yielding a standard multinomial logit (MNL) model for consumer choice.[7] Following standard practice, we normalize the utility of the outside option $(j = 0)$ to zero for all consumer locations. The probability $s_{j\ell\tau}^t$ that a consumer arriving at location ℓ at (t, τ) chooses store j is then

$$s_{j\ell\tau}^t(\boldsymbol{\psi}; \boldsymbol{\beta}) = \frac{e^{V_{j\ell}(\boldsymbol{\beta})}}{1 + \sum_{j' \in \mathcal{J}_\tau^t(\boldsymbol{\psi})} e^{V_{j'\ell}(\boldsymbol{\beta})}} \cdot \mathbf{1}_{\{j \in \mathcal{J}_\tau^t(\boldsymbol{\psi}) \cup \{0\}\}}, \qquad (1)$$

where $\{0\}$ represents the outside option available to all consumers. Finally, the aggregate demand for an entrant $j \in \mathcal{J}^+(\boldsymbol{\psi})$ at time (t, τ) is obtained by summing over all consumer locations:

$$D_{j\tau}^t(\boldsymbol{\psi}; \boldsymbol{\alpha}, \boldsymbol{\beta}) = \sum_{\ell \in \mathcal{L}} \lambda_{\ell\tau}^t(\boldsymbol{\alpha}) \cdot s_{j\ell\tau}^t(\boldsymbol{\psi}; \boldsymbol{\beta}). \qquad (2)$$

To ease the computational burden, we assume that consumers are not willing to travel beyond 2 kilometers, which moderates the size of their choice sets. Under this assumption, when computing demand $D_{j\tau}^t$, we aggregate only over the locations ℓ that are within the 2-kilometer radius of store j.

3.2 Sellers' Profit and Entry

The supply side of our model characterizes sellers' market entry decisions as a one-shot game based on expected profitability. We adopt a static-entry framework in the spirit of Bresnahan and Reiss (1991) and Berry (1992). This setup is appropriate in our setting given the platform's relatively short operating horizon and our focus on cross-sectional variation across a large number of small sellers.[8]

Each seller $j \in \mathcal{J}$ has random inventory $Q_{j\tau}$ available in period τ, representing surplus food.[9] To capture the empirical prevalence of zero-inventory days, we model $Q_{j\tau}$ using a hurdle model (Cragg, 1971), using a truncated Poisson to model non-zero inventory. Specifically, with probability μ the seller has no surplus inventory on day τ:

$$\Pr(Q_{j\tau} = 0) = \mu.$$

---

[7]The MNL model exhibits the independence of irrelevant alternatives (IIA) property, which is known to have unrealistic implications for consumer behavior (Train, 2009). To some extent, this is mitigated in our empirical application due to the spatial heterogeneity captured by the demand model (i.e., variation in consumer-seller distances). This allows for more realistic substitution patterns across stores based on their geographic proximity, by accounting for the fact that consumers are more likely to substitute between nearby stores than distant ones.

[8]Fully dynamic entry models have typically been used to study firm entry/exit over years or decades (e.g, Jia (2008); Collard-Wexler (2013)). Dynamic entry models also pose computational challenges due to the need to solve a Bellman equation whose state spaces grows exponentially with the number of sellers (Pakes et al., 2007; Aguirregabiria and Mira, 2007), making estimation infeasible for games with many players, as in our setting.

[9]Sellers rarely release inventory more than once per day: Mid-day replenishment occurs on only 2.6% of store-days across all markets.

For simplicity, we assume all stores in the market have the same zero-inventory probability, μ. Conditional on positive inventory, $Q_{j\tau}$ follows a Poisson distribution, with its rate depending on the exponential of seller characteristics $\mathbf{x}_j^Q$ and parameter vector $\boldsymbol{\zeta}$:

$$Q_{j\tau} \mid Q_{j\tau} > 0 \ \sim \ \text{Poisson}\left(\exp\left(\zeta_0 + \boldsymbol{\zeta}^\top \mathbf{x}_j^Q\right)\right).$$

The exponential ensures the Poisson rate is positive. We write $H_j(\mu, \boldsymbol{\zeta})$ to denote the inventory distribution for seller j. Our assumption that sellers' surplus inventory is exogenous is mild because the surplus market represents only a small fraction the seller's total revenue, making it unlikely that sellers would adjust major production decisions in the primary market in anticipation of surplus market sales.[10]

The retail value of seller j's bag is denoted by R_j. Let $\bar{p}(R_j)$ be seller j's price in the surplus market, typically a fixed fraction of the retail value (e.g., $1/3$). Consistent with the platform's current practice of setting discount rates uniformly across all sellers, we assume $\bar{p}(R_j)$ is exogenous from the seller's perspective. The period-τ sales for an entrant j is then given by $\min\{D_{j\tau}(\boldsymbol{\psi}; \boldsymbol{\alpha}, \boldsymbol{\beta}), Q_{j\tau}(\boldsymbol{\zeta})\}$, where $D_{j\tau}(\boldsymbol{\psi}; \boldsymbol{\alpha}, \boldsymbol{\beta}) = \sum_{t \in \mathcal{T}} D_{j\tau}^t(\boldsymbol{\psi}; \boldsymbol{\alpha}, \boldsymbol{\beta})$ is the aggregate demand for seller j in period τ. The $\min\{\}$ operator captures the constraint that sales cannot exceed either available inventory or realized demand.

Sellers' entry decisions are shaped by their fixed cost of entry and marginal (i.e., per-bag) cost. Seller j's marginal cost is parameterized by $\boldsymbol{\theta}^c$, where

$$c_j(\boldsymbol{\theta}^c) := \theta_0^c + (\boldsymbol{\theta}^c)^\top \mathbf{x}_j^c + \varepsilon_j^c$$

and $\mathbf{x}_j^c$ is a vector of observable seller characteristics (e.g., seller ratings in the primary market). The term ε_j^c represents Normally distributed seller-specific shocks, assumed to be zero-mean with standard deviation σ^c. The marginal cost c_j may capture transaction costs or opportunity costs from releasing the inventory to the platform. The seller's expected profit contribution before fixed costs is then

$$\mathbb{E}[\pi_j(\boldsymbol{\psi}; \boldsymbol{\alpha}, \boldsymbol{\beta}, \boldsymbol{\zeta}, \boldsymbol{\theta}^c)] := (\bar{p}(R_j) - c_j(\boldsymbol{\theta}^c)) \cdot \sum_{\tau \in \mathcal{T}} \mathbb{E}[\min\{D_{j\tau}(\boldsymbol{\psi}; \boldsymbol{\alpha}, \boldsymbol{\beta}), Q_{j\tau}(\boldsymbol{\zeta})\}].$$

In addition to marginal costs, sellers incur a fixed cost to enter the market. The market is divided into disjoint geographic *segments* $m \in \mathcal{M}$ (e.g., zip codes), with each seller belonging to exactly one segment. Let $\mathcal{J}_m$ denote the set of all potential sellers in segment m. Each segment m is characterized

---

[10]Empirically, we observe the mean daily revenue of sellers in the marketplace to be \$5 to \$19, which is a small fraction of typical daily revenue in the primary market.

by a vector of attributes $\mathbf{v}_m$. The fixed entry cost for segment m is then given by

$$F_m(\boldsymbol{\theta}^F) = \theta_0^F + (\boldsymbol{\theta}^F)^\top \mathbf{v}_m + \varepsilon_m^F,$$

where ε_m^F are Normally distributed zero-mean segment-level shocks, with standard deviation σ^F. Finally, we can write seller j's total profit as a function of their binary entry decision ψ_j as:

$$\mathbb{E}[\Pi_j(\boldsymbol{\psi}; \boldsymbol{\alpha}, \boldsymbol{\beta}, \boldsymbol{\zeta}, \boldsymbol{\theta})] := \psi_j \cdot \left[\mathbb{E}[\pi_j(\boldsymbol{\psi}; \boldsymbol{\alpha}, \boldsymbol{\beta}, \boldsymbol{\zeta}, \boldsymbol{\theta}^c)] - F_m(\boldsymbol{\theta}^F) \right]. \tag{3}$$

Note the expectation in seller j's profit function is taken over the distributions of inventory quantity, consumer arrivals, and idiosyncratic shocks in consumer utility.

3.3 Market Equilibrium

Because each seller's expected profit $\mathbb{E}[\Pi_j(\cdot)]$ depends on the decisions of other sellers, all sellers' entry decisions are the outcome of a strategic entry game, played within each segment $m \in \mathcal{M}$. Let $\boldsymbol{\psi}_m = [\psi_j : j \in \mathcal{J}_m]$. We formalize the definition of equilibrium in the entry game next:

Definition 1. *For each segment* $m \in \mathcal{M}$, *a strategy profile* $\boldsymbol{\psi}_m$ *is an equilibrium if and only if* $\mathbb{E}[\Pi_j(\boldsymbol{\psi}; \boldsymbol{\alpha}, \boldsymbol{\beta}, \boldsymbol{\zeta}, \boldsymbol{\theta})] \geq 0$.

A market equilibrium in our model consists of seller entry decisions, consumer choice probabilities, and expected sales. To ensure tractability in estimation of the entry game, we introduce two key assumptions.

Assumption 1 (**Segment Competition**)**.** *In the entry game, sellers assume they only compete against other sellers in their geographic segment.*

Assumption 1 significantly improves tractability of estimation. It implies that sellers ignore the potential entry of sellers outside their own market segment when forming beliefs about expected profit, which is reasonable given that food retailers primarily compete locally with nearby establishments.

Assumption 2 (**Cost-Based Entry**)**.** *Prior to entry, each seller* j *in segment* m *only knows their own cost* c_j *and the segment entry cost* F_m *when they enter, i.e., sellers form profit beliefs by taking expectations over demand* $D_{j\tau}$, *quantity* $Q_{j\tau}$, *and bag value* V_j.

Assumption 2 guarantees a unique, threshold-based equilibrium in each segment's entry game that depends only on the sellers' marginal costs c_j. While it is stronger than Assumption 1, the guarantee of a unique equilibrium eliminates ambiguity in our counterfactuals by avoiding the multiplicity of equilibria

that typically plague entry games (Ciliberto and Tamer, 2009). The assumption can be interpreted as sellers having no prior information about the distribution of their competitors characteristics, which is reasonable given our focus on a large number of small sellers and the relative novelty of the surplus market; a similar assumption is used in Lee and Musolff (2023).

Assumptions 1 and 2 lead to the following characterization of the entry game:

Proposition 1 (**Unique Entry Equilibrium**). *Under Assumptions 1 and 2, there exists a unique entry equilibrium characterized by a set of threshold costs $c_1^*, c_2^*, \ldots, c_{|\mathcal{M}|}^*$ such that seller $j \in \mathcal{J}_m$ enters market segment $m \in \mathcal{M}$ if and only if $c_j \leq c_m^*$.*

The existence of a unique threshold equilibrium follows in a straightforward manner from the monotonicity of sellers' expected profit in their marginal cost c_j (proof in Appendix C). The market equilibrium is defined by two conditions: First, given the set of entering sellers, consumers choose among the available products to maximize utility. Second, given the induced choice probabilities and entry decisions of other sellers, each seller enters if and only if doing so is profitable. We impose these equilibrium conditions explicitly in estimation, described next.

4 Demand Estimation: Consumer Arrival and Choice

Section 4.1 specifies the demand-side model. Section 4.2 discusses the main endogeneity challenge in our setting and and describes the instrument we use to address it.

4.1 Specification

We let the number of potential consumers arriving at a location ℓ hour t on date τ be given by

$$\lambda_{\ell\tau}^t(\boldsymbol{\alpha}) = \alpha_0 + \alpha_1 \cdot PopulationDensity_\ell + \alpha_2 \cdot Weekend_\tau + \alpha_3 \cdot Income_\ell.$$

This specification accounts for demographic and temporal factors that influence consumer arrivals. For simplicity, arrivals depend only on the aggregated time period τ, but not t. For consumer choice, the deterministic component of utility for seller $j \in \mathcal{J}_\tau^t(\boldsymbol{\psi})$ at location ℓ is specified as:

$$V_{j\ell}(\boldsymbol{\beta}) = \beta_0 + \beta_1 \cdot f(PlatformRating_j, \nu) + \beta_2 \cdot Distance_{j\ell} + \beta_3 \cdot BagPrice_j + RetailPrice_j^\gamma + \delta_\ell + \xi_j.$$

Here, $PlatformRating_j$ denotes the store's platform rating, reflecting perceived quality. We specify $f(PlatformRating_j, \nu) = e^{\nu \cdot PlatformRating_j}$, which allows ratings to influence consumer utility non-linearly. Our assumption that consumer utility is convex in $PlatformRating$ is supported by the observed linearity in the sale probability shown in Figure 2. The term $Distance_{j\ell}$ is the Euclidean

16

distance between consumer location ℓ and seller j, capturing consumers' travel costs; we assume all consumers arrive at the centroid of a census tract. $BagPrice_j$ is the discounted price on the platform and $RetailPrice_j$ is the original retail value in the primary market. The exponent $\gamma \in (0, 1)$ is a hyper-parameter representing consumers' mental discounting of the bag's value, potentially due to reduced freshness, as most pick-up windows occur in the late afternoon or early evening. To mitigate multi-collinearity between $BagPrice_j$ and $RetailPrice_j$, γ is constrained to be strictly less than 1. Finally, δ_ℓ denotes the census tract fixed effect and ξ_j captures unobserved demand shocks for seller j.

Identification of $\boldsymbol{\alpha}$ and $\boldsymbol{\beta}$ is supported through spatial variation in consumer demographics and cross-sectional variation in store characteristics, respectively. However, because we do not observe consumer arrivals and market shares separately, the variation in aggregate sales across stores only jointly identifies $\boldsymbol{\alpha}$ and $\boldsymbol{\beta}$. Two additional sources of variation allow for disentanglement and precise identification of both parameters. First, the hourly-level inventory data allow us to observe when products stock out at different times during the day, which creates exogenous variation in consumers' choice sets and helps pin down $\boldsymbol{\beta}$.[11] For example, when a popular store stocks out, the re-distribution of demand among remaining options reveals substitution patterns that identify the choice model. Additionally, the limited search radius of consumers induces spatial variation in consumers' choice sets, which further separates $\boldsymbol{\alpha}$ from $\boldsymbol{\beta}$ by creating variation in sales that can only be explained by differences in arrival rates, rather than preferences.

4.2 An Instrument for Consumer-Seller Distances

Our demand model captures spatial heterogeneity in consumer preferences through the variable $Distance_{j\ell}$. The coefficient β_2 represents consumers' distance sensitivity, which one expects to be negative (i.e., consumers are less likely to purchase from more distant stores). However, consumer–seller distances are likely endogenous because sellers' geographic locations and decision to enter the surplus market may be influenced by unobserved seller characteristics. For example, stores may locate in popular commercial areas based on proprietary market research or historic sales patterns. These stores may attract higher demand despite being farther from residential neighborhoods, which would lead to attenuation bias in β_2. Additionally, stores located far from consumers may experience lower sales in the primary market, which increases the probability that these outlets accumulate excess food and subsequently enter the surplus food marketplace. Consequently, the sample of marketplace participants is likely to over-represent stores with greater travel distances, biasing β_2 away from 0.

Our model explicitly accounts for the endogeneity of consumer–seller distances, an identification chal-

---

[11]See Musalem et al. (2010) and Conlon and Mortimer (2013) for prior work that also uses stock-outs to identify consumer choice models.

lenge that warrants careful attention in spatial demand estimation but has until recently been overlooked (Cao et al., 2024). In particular, we address the endogeneity of distance through use of instrumental variables within a generalized method of moments (GMM) framework, following standard practice in demand estimation (Berry et al., 1995; Nevo, 2001). Given a set of valid instruments $\{Z_{j\ell}^k : k = 1, \ldots, K\}$, the key identifying assumptions are the orthogonality conditions

$$\mathbb{E}[Z_{j\ell}^k \cdot \xi_j(\boldsymbol{\alpha}, \boldsymbol{\beta})] = 0, \quad k = 1 \ldots, K, \tag{4}$$

which states that each instrument is uncorrelated with the structural error term ξ_j. These moment conditions ensure that variation in the endogenous regressors (i.e., distance) induced by the instruments is independent of unobserved demand shocks, allowing for consistent estimation of the distance sensitivity β_2.

The GMM optimization problem amounts to finding parameters $(\boldsymbol{\alpha}, \boldsymbol{\beta})$ such that the sample analog of the expectation in (4) in is minimized. The standard approach to computing the demand shocks ξ_j as a function of the parameter estimates $(\boldsymbol{\alpha}, \boldsymbol{\beta})$ is the "share inversion" approach proposed by Berry et al. (1995). However, this approach does not work in our setting because consumers' choice sets vary over time and the market share from each consumer location ℓ is unobserved. We instead recover ξ_j by solving a non-linear optimization problem – additional details are provided in Appendix E.

To be a valid instrument, $Z_{j\ell}^k$ must be correlated with $Distance_{j\ell}$ (relevance), and uncorrelated with the error term ξ_j (exclusion). We construct instruments that plausibly satisfy both conditions by using the locations of historical landmarks – specifically, each market's city hall and courthouses. The relevance condition is supported by the fact that these landmarks were located in the early stages of urban development (i.e., 19th century) and their locations were influenced by the same factors that also shaped the emergence of commercial districts, such as historic land-use patterns and regulations. As a result, the locations of present-day food retailers are likely to be spatially correlated with these landmarks, satisfying the relevance condition. However, the locations of these landmarks are also plausibly exogenous to modern demand shocks since they predate contemporary factors that shape consumer preferences, as well as platform-specific demand shocks, thus satisfying the exclusion condition. Appendix E.2 provides details of instrument construction and strength tests.

5 Supply Estimation: Seller Inventory and Entry Costs

We estimate the supply-side of the model (i.e., sellers' entry costs) by matching the predicted and empirical number of entrants in each market segment, following Berry (1992). Doing so is computationally challenging in our setting: Because seller entry is modeled explicitly as the outcome of a

discrete game, the equilibrium number of entrants under the model cannot be expressed in closed form, which makes continuous optimization within a standard generalized method of moments (GMM) framework inapplicable. Additionally, our model lacks a tractable likelihood function that describes the number of entrants, which precludes likelihood-based estimators (e.g., as used by Seim (2006) for market entry). We address this by proposing a novel estimator for sellers' cost parameters based on integer optimization.

Section 5.1 specifies sellers' fixed and marginal cost functions. Section 5.2 presents an estimator for recovering the cost parameters based on the method of moments. Section 5.3 describes how the estimator can be expressed exactly as an integer optimization model, with technical details relegated to the Appendix.

5.1 Specification

On the supply-side, the key parameters to be estimated are the inventory parameters $(\boldsymbol{\mu}, \boldsymbol{\zeta})$, the fixed and marginal cost parameters $\boldsymbol{\theta} = (\boldsymbol{\theta}^F, \boldsymbol{\theta}^c)$, and the standard deviations of the cost shocks $\boldsymbol{\sigma} = (\sigma^F, \sigma^c)$. We suppress dependence on demand-side parameters below. First, we specify the inventory as

$$\Pr(Q_{j\tau} = 0) = \mu, \quad Q_{j\tau} \,\big|\, Q_{j\tau} > 0 \sim \text{Poisson}\big(\exp(\zeta_0 + \zeta_1 \cdot GoogleRating_j)\big), \quad \forall j \in \mathcal{J}, \ \tau \in \mathcal{T}.$$

Note that because the inventory $Q_{j\tau}$ depends only on exogenous seller characteristics and we observe the daily quantities directly, the parameters $\boldsymbol{\mu}$ and $\boldsymbol{\zeta}$ can be estimated through a maximum likelihood approach using the daily store-level inventory data; the technical details are straightforward and omitted. Next, we specify sellers' fixed and marginal cost[12] functions:

$$F_m(\boldsymbol{\theta}^F) = \theta_0^F + \theta_1^F \cdot MedianHomeValue_m + \varepsilon_m^F,$$
$$c_j(\boldsymbol{\theta}^c) = \theta_0^c + \theta_1^c \cdot GoogleRating_j + \theta_2^c \cdot PopulationDensity_j + \theta_3^c \cdot HoursOpen_j$$
$$+ \theta_4^c \cdot \log(RatingCount_j) + \theta_5^c \cdot CoffeeShopIndicator_j + \theta_6^c \cdot StyleIndicator_j + \varepsilon_j^c.$$

We use zip code boundaries to define the geographic segments $m \in \mathcal{M}$. The variable $MedianHomeValue_m$ denotes the median home value in geographic segment m and serves as a proxy for local affluence, which may influence staff wages and brand considerations.

The variables $GoogleRating_j$ and $\log(RatingCount_j)$ capture store quality and popularity in the primary market, which may influence operational efficiency. $PopulationDensity_j$ is the population density of

---

[12]The fixed cost of joining the platform, F_m, may include staff training, new sales hardware, potential brand and reputational costs from selling surplus food, and the annual platform membership fee, typically $89 in the U.S. (Wu and Duarte, 2024). The marginal cost, c_j, captures transaction and opportunity costs from listing surplus inventory on the platform.

the geographic segment in which the store is located, averaged over census tracts. The variables *HoursOpen_j* is the total weekly hours of operation, and *CoffeeShopIndicator_j* is a dummy to capture systematic differences in cost structures across store types. The variable *StyleIndicator_j* categorizes stores as "upscale" or "basic", and is constructed using natural language processing based on Google's text description of the store (see Appendix F.2). The variables described above provide variation within and across segments, enabling the identification of $\boldsymbol{\theta}^F$ and $\boldsymbol{\theta}^c$.

5.2 Moment-Based Estimator

The cost parameters $\boldsymbol{\theta} = (\boldsymbol{\theta}^F, \boldsymbol{\theta}^c)$ can be estimated by matching empirical and model-predicted moments within a simulated method of moments framework (McFadden, 1989; Pakes and Pollard, 1989). Following Berry (1992), we use the number of stores entering each segment as our primary moment condition. For notational clarity, we write the estimation problem for a single set of simulated shocks. Let $(\boldsymbol{\varepsilon}_m^F, \boldsymbol{\varepsilon}_j^c)$ be the simulated shocks under the parameter $\boldsymbol{\sigma}$. Let N_m denote the observed number of entrants in segment m, and let $\hat{N}_m(\boldsymbol{\theta})$ represent the model-predicted number of entrants under parameters $\boldsymbol{\theta}$. Using the expression for $\mathbb{E}[\Pi_j]$ from (3), the moment optimization problem can be written as

$$\underset{\boldsymbol{\theta}}{\text{minimize}} \quad \sum_{m \in \mathcal{M}} \left| N_m - \hat{N}_m(\boldsymbol{\theta}) \right| \tag{5}$$

$$\text{subject to} \ \ \hat{N}_m(\boldsymbol{\theta}) = \sum_{j \in \mathcal{J}_m} \mathbf{1} \left\{ (\bar{p}(R_j) - c_j(\boldsymbol{\theta}^c)) \cdot \sum_{\tau \in \mathcal{T}} \mathbb{E}[\min\{D_{j\tau}(\boldsymbol{\psi}), Q_{j\tau}\}] \geq F_m(\boldsymbol{\theta}^F) \right\}.$$

We adopt the L_1-norm in the objective function for computational simplicity when reformulating the estimator as an integer optimization model in the next section.

The typical approach to solving estimators of the form (5) is to use a nested fixed-point (NFXP) algorithm (Rust, 1987; Bajari et al., 2010) within a simulated method of moments framework. In short, these algorithms optimize the moment condition by iterating through two loops: An outer loop that searches over values of the structural parameters $\boldsymbol{\theta}$ (e.g., within a grid), and an inner loop that solves for the relevant equilibrium at each parameter instance. If necessary, shock distribution parameters (e.g., $\boldsymbol{\sigma}$) can also be estimated through a grid search in another outer loop, prior to simulating shocks. See Lee and Musolff (2023) for an example of an NFXP algorithm implemented within a market entry context, and Appendix F.5 for details of an NFXP algorithm applied to the estimator (5).

The challenge with NFXP algorithms is that they are well-known to become computationally intractable as the number of parameters increases (Su and Judd, 2012), which in our setting can make estimation nonviable for models with even a modest number ($\leq$ 5) of cost parameters. Instead of using an

NFXP algorithm, we propose an alternative solution technique that leverages the paradigm of integer optimization (Wolsey, 2020), described next.

5.3 Method of Moments via Integer Optimization

We provide a brief overview of our method of moments via integer optimization (MMIO) approach here and provide additional details in Appendix F. Intuitively, the binary nature of sellers' equilibrium strategies allows us to use discrete variables to endogenize sellers' entry decisions within the estimator. This results in an optimization problem that *jointly* searches over possible equilibria and the cost parameters $(\boldsymbol{\theta}^F, \boldsymbol{\theta}^c)$, instead of nesting them in separate steps, as in NFXP methods.[13] This difference in solution technique yields enormous computational advantages over NFXP, as demonstrated through numerical experiments on synthetic data in Appendix F.

Our approach proceeds in two steps. First, we use a random forest to construct a pool of "candidate equilibria" for the estimator to search over in tandem with the cost parameters. This pre-processing step avoids searching over all possible $2^{|\mathcal{J}_m|}$ equilibria in each market segment by focusing only on those that are most plausible based on the data. We refer the readers to Appendix F.1 for details of candidate equilibria generation.

Second, we solve the estimator (5) by expressing it as an integer optimization problem. Despite narrowing down the set of candidate equilibria in the first step, the full optimization problem remains challenging when the number of sellers $|\mathcal{J}|$ or market segments $|\mathcal{M}|$ are large, because each seller introduces a pair of equilibrium entry conditions that must be enforced during estimation, leading to a large number of constraints in the optimization model. We address this by developing an iterative solution technique in the spirit of "cutting plane" methods that are commonly used to solve large-scale integer optimization problems (Geoffrion and Marsten, 1972; Wolsey and Nemhauser, 1999; Wolsey, 2020). Intuitively, the technique focuses on a small set of sellers and iteratively generates equilibrium conditions for additional sellers on-the-fly, which drastically improves computational performance. Our method is general enough to have applications beyond our specific context of surplus food marketplaces, and to our knowledge is the first use of integer optimization to estimate player payoffs within a discrete game.

---

[13]Similar to Su and Judd (2012), our estimator involves enforcing equilibrium conditions within a mathematical program. However, their framework focuses on continuous decisions and requires closed-form equilibrium conditions, which are typically unavailable in discrete games.

Table 2: Example Performance of MMIO and NFXP Estimators.

Segments	$\|\boldsymbol{\theta}^c\|$	$\|\boldsymbol{\theta}^F\|$	Stores	Runtime (min)	RRMSE ($\boldsymbol{\theta}^c$)	RRMSE ($\boldsymbol{\theta}^c$)
				MMIO		
10	2	2	449	6	0.42	0.31
10	11	2	449	86	0.08	0.64
				NFXP		
10	2	2	449	610	0.18	0.26
10	11	2	449	1202	0.37	0.69

Notes: $\|\boldsymbol{\theta}^c\|$ and $\|\boldsymbol{\theta}^F\|$ denote the dimensionality of the marginal and fixed cost parameters (including the intercept), respectively. Estimation accuracy is assessed using the Relative Root Mean Square Error (RRMSE), computed relative to the true initialized values of $\boldsymbol{\theta}^c$ and $\boldsymbol{\theta}^F$. All results are based on the shock standard deviations $(\sigma^c, \sigma^F) = (0.05, 0.05)$.

6 Estimation Results

This section presents estimation results for both the demand- and supply-side of the model for all four U.S. markets. A map of the study regions and key summary statistics are provided in Appendix B.1.

6.1 Parameter Estimates

Table 3 reports the estimated coefficients from the consumer arrival and choice models. We find significant heterogeneity in consumer preferences with respect to *PlatformRating* and *Distance*, discussed more in Section 6.3.

Table 4 reports the parameter estimates that determine sellers' marginal ($\boldsymbol{\theta}^c$) and fixed costs ($\boldsymbol{\theta}^F$). Combined with the covariate means (Table 11 in Appendix B.1), the estimates allow us to recover the average marginal cost in each market. The marginal cost of one bag is approximately \$10.26 in Manhattan, \$10.18 in San Francisco, \$13.97 in Boston, and \$14.13 in Seattle, indicating substantial cross-city heterogeneity. For all four cities, the average costs far exceed the observed bag prices (Table 10 in Appendix B.1), suggesting that high marginal costs may help explain limited market entry by food retailers. With respect to fixed costs, we estimate them to be relatively small and comparable to the magnitude of the prorated annual platform membership fee, which is approximately \$17 per store for a 10-week period. The coefficient on *MedianHomeValue* is estimated to be zero in all markets.

Table 3: Estimated Coefficients for Consumer Arrival and Choice Model.

	Manhattan	San Francisco	Boston	Seattle
Consumer arrival ($\boldsymbol{\alpha}$)				
Intercept	0.98 (0.08)	1.77 (0.07)	0.57 (0.06)	1.99 (0.07)
PopulationDensity	1.38 (0.09)	0.75 (0.06)	1.36 (0.06)	2.10 (0.05)
Weekend	-1.98 (0.08)	-1.23 (0.07)	-2.28 (0.06)	-1.82 (0.06)
Income	0.54 (0.07)	1.85 (0.05)	0.14 (0.07)	1.48 (0.07)
Consumer choice ($\boldsymbol{\beta}$)				
Intercept	1.58 (0.04)	1.02 (0.06)	1.15 (0.10)	-0.42 (0.14)
PlatformRating	1.74 (0.03)	0.52 (0.02)	1.67 (0.03)	0.90 (0.03)
Distance	-0.65 (0.04)	-1.98 (0.05)	-1.00 (0.07)	-2.02 (0.11)
BagPrice	-1.79 (0.04)	-1.59 (0.05)	-2.09 (0.07)	-2.19 (0.10)
Scale parameter (ν)	0.50	0.44	0.48	0.46
Census tract FE (δ_ℓ)	YES	YES	YES	YES
IV	YES	YES	YES	YES

Notes: All specifications include census tract fixed effects (FE). Instruments (IV) are described in Section 4. Standard errors, shown in parentheses, are estimated through subsample bootstrapping and rescaling. ν is the scale parameter for the PlatformRating covariate. The mental discounting hyperparameter γ is set to 0.9 for all markets. *PopulationDensity* is measured as persons per square meter and calculated at the census tract level. *Weekend* equals 1 on weekends and 0 otherwise. *Income* denotes the median household income of a census tract, measured in units of USD 100,000.

Table 4: Estimated Coefficients for Sellers' Cost Functions.

	Manhattan	San Francisco	Boston	Seattle
Marginal costs ($\boldsymbol{\theta}^c$)				
Intercept ($)	0.44	9.43	0.74	1.24
GoogleRating	0.00	0.00	1.85	1.58
PopulationDensity	0.00	3e−03	0.00	0.00
HoursOpen	0.00	8e−03	9e−03	0.06
$\log(RatingCount)$	1.74	0.05	0.09	0.00
CoffeeShopIndicator ($)	0.54	0.00	8.20	0.00
StyleIndicator ($)	0.93	0.00	2.63	4.95
Fixed costs ($\boldsymbol{\theta}^F$)				
Intercept ($)	10.25	24.84	27.61	16.97
MedianHomeValue	0.00	0.00	0.00	0.00

Notes: Small coefficients (absolute value < 0.01) are reported in scientific notation. *PopulationDensity* is measured in persons per square kilometer and is calculated at the market-segment (ZIP-code) level. *HoursOpen* denotes total weekly operating hours. Indicator variables are defined as follows: *CoffeeShopIndicator* = 1 if the store is a coffee shop (0 otherwise); *StyleIndicator* = 1 if upscale (0 if basic). *MedianHomeValue* is measured in millions of U.S. dollars. Fixed cost estimates correspond to the pro-rated entry cost for the number of days in our sample: 64 days for Manhattan, San Francisco, and Boston, and 45 days for Seattle.

Lastly, Table 5 reports the hurdle model estimates for sellers' random inventory, and Figure 4 compares the fit of the inventory model with empirical data based on seller-day observations.

Table 5: Parameter Estimates for Inventory Hurdle Model.

	Manhattan	**San Francisco**	**Boston**	**Seattle**
Zero probability, μ	0.51 (0.03)	0.57 (0.04)	0.50 (0.06)	0.67 (0.04)
Intercept, ζ_0	2.71 (0.85)	-3.55 (2.43)	-5.85 (5.72)	3.95 (3.33)
Google Rating, ζ_1	-0.31 (0.19)	1.02 (0.56)	1.54 (1.33)	-0.65 (0.73)

Notes: Standard errors (in parentheses) are obtained by bootstrapping with 1,000 replications, resampling at the store level.

Figure 4: Inventory Hurdle Model Fit.

| Manhattan | San Francisco | Boston | Seattle |
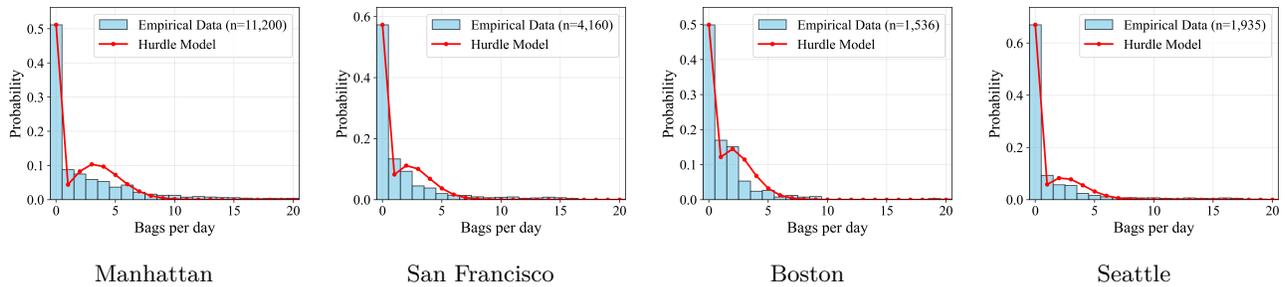
Notes: Parameter n denotes number of store-day observations.

6.2 Model Fit

Figure 5 illustrates the model fit in terms of seller-level market shares, with observed shares calculated from realized sales. The RMSE ranges from 0.002 to 0.021 across the four markets, indicating strong in-sample predictive performance. We use the log scale in Figure 5 because the distribution of market shares is skewed.

Figure 5: Observed vs. Predicted Market Shares.
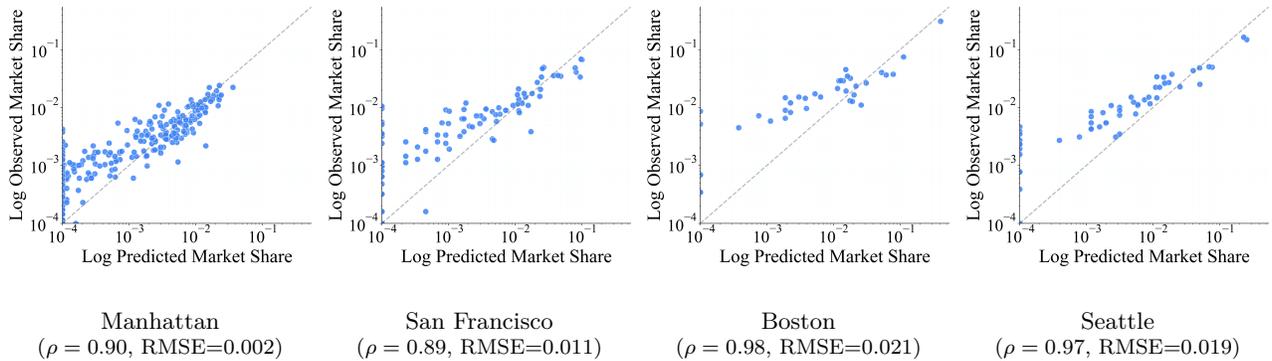
| Manhattan | San Francisco | Boston | Seattle |
| ($\rho = 0.90$, RMSE=0.002) | ($\rho = 0.89$, RMSE=0.011) | ($\rho = 0.98$, RMSE=0.021) | ($\rho = 0.97$, RMSE=0.019) |

Notes: Observed vs predicted market share (log-log, same scale) across markets. Reported ρ values denote correlation and RMSE values measure model fit, both using original untransformed market share values.

We combine the estimated consumer demand, inventory, and cost parameters to compute sellers' profit functions. Using these profit functions, we simulate the full market equilibrium under the estimated structural model. We assess goodness-of-fit by comparing the predicted and observed number of entrants per market segment (Figure 6), as well as the predicted and observed sales volumes (Figure 7). The fit appears reasonable given the small number of entrants in each market segment.

Figure 6: Observed vs. Predicted Entrant Count per Segment.

Manhattan	San Francisco	Boston	Seattle
($\rho = 0.55$, RMSE=2.89)	($\rho = 0.66$, RMSE=1.37)	($\rho = 0.42$, RMSE=0.93)	($\rho = 0.57$, RMSE=1.73)
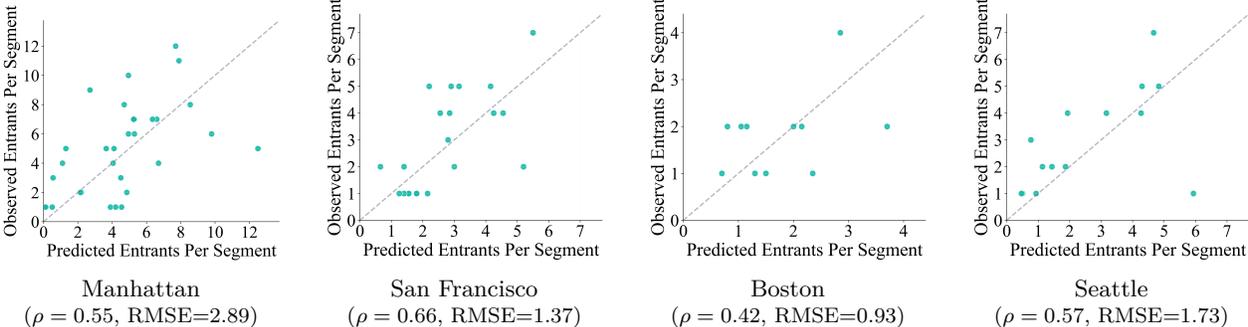
Figure 7: Observed vs. Predicted Aggregate Sales by Segment.

Manhattan	San Francisco	Boston	Seattle
($\rho = 0.94$, RMSE=195.6)	($\rho = 0.98$, RMSE=38.2)	($\rho = 0.97$, RMSE=42.5)	($\rho = 0.98$, RMSE=27.5)
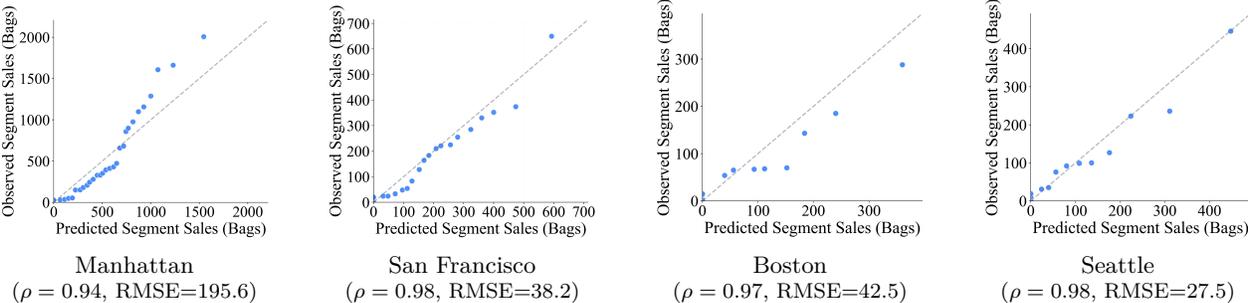
Notes: One outlier not shown in each market.

6.3   How Do Consumer Preferences Vary by Urban Environment?

We now address our first research question: *How do consumer preferences in surplus food marketplaces vary across urban environments?* Table 3 reveals clear differences in how consumers across the four markets weigh quality and travel costs. We use these estimates to compute the dollar-equivalent decrease in price that yields the same change in consumer utility as a one-star increase in seller rating, and the same for a one-kilometer decrease in travel distance. This normalization allows us to directly compare across the four urban centers in our sample.

In all four markets, a one-star improvement in a seller's rating is equivalent to a substantial price decrease, although the magnitude varies: Manhattan and Boston are most responsive to ratings ($5.86 and $4.11 per star, respectively), while the effect is more modest in Seattle ($2.12) and San Francisco

($1.33). Interestingly, the ordering of the four markets is exactly reversed when considering travel costs: San Francisco and Seattle consumers experience the largest disutility from each additional kilometer ($1.25 and $0.92, respectively), whereas travel costs are lower in Boston ($0.48) and Manhattan ($0.36).

Figure 8 visualizes consumer preferences in dollar-equivalents. We offer the following reasoning for the depicted behavior. In the denser and more accessible markets of Manhattan and Boston, low travel costs expand consumers' effective choice sets, allowing them to compare more sellers easily. This intensifies quality competition and leads sellers to become more quality-focused, which is reflected in consumers exhibiting higher rating sensitivity in those markets. The opposite is true in San Francisco and Seattle, where higher travel costs force consumers to focus on nearby sellers, softening the role of ratings. These results suggest the nature of seller competition is materially influenced by the urban environment in which the market operates – in particular, sellers in low travel-cost cities must maintain strong on-platform reputations to thrive in the marketplace.

Figure 8: Dollar-Equivalents of Platform Ratings and Seller Distance.
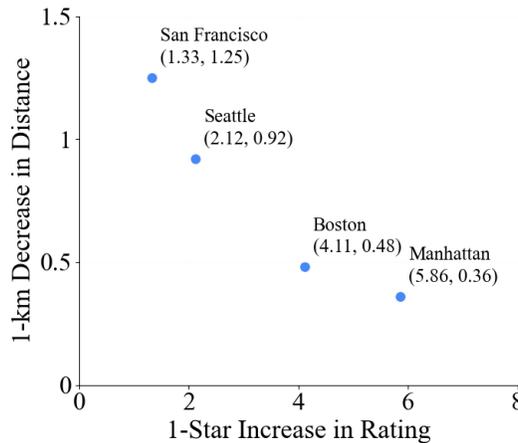
Notes: Consumer preference for quality (*PlatformRating*) improvement and travel cost (*Distance*) reduction in dollar-equivalents across markets. Each marker represents a city, with coordinates indicating the dollar value of a one-star increase in rating and a one-kilometer increase in distance. For ratings, the dollar equivalent is computed from the mean rating in each market.

7 Counterfactuals

In this section, we use our estimated model to conduct two counterfactual analyses, corresponding to our second and third research questions. *Do demand- or supply-side effects dominate in response to market-wide price changes? How does permitting seller price competition impact seller entry and aggregate sales volume?*

7.1 Do Demand- or Supply-side Effects Dominate Pricing?

We first consider the status-quo policy where the platform sets a uniform price ratio for all sellers in each market. We simulate market equilibria over a grid of uniform price ratios, varying in 5-percentage-point increments above and below the status quo ratio of 33%. At each price ratio, we recompute the market equilibrium and simulate aggregate sales and the number of entrants, following Algorithms 1 and 2 respectively. We identify the optimal price ratio under the objective of maximizing aggregate sales. Results are presented in Figure 9 and Table 6.

Figure 9: Equilibrium Entry and Sales Under Uniform Price Ratios.
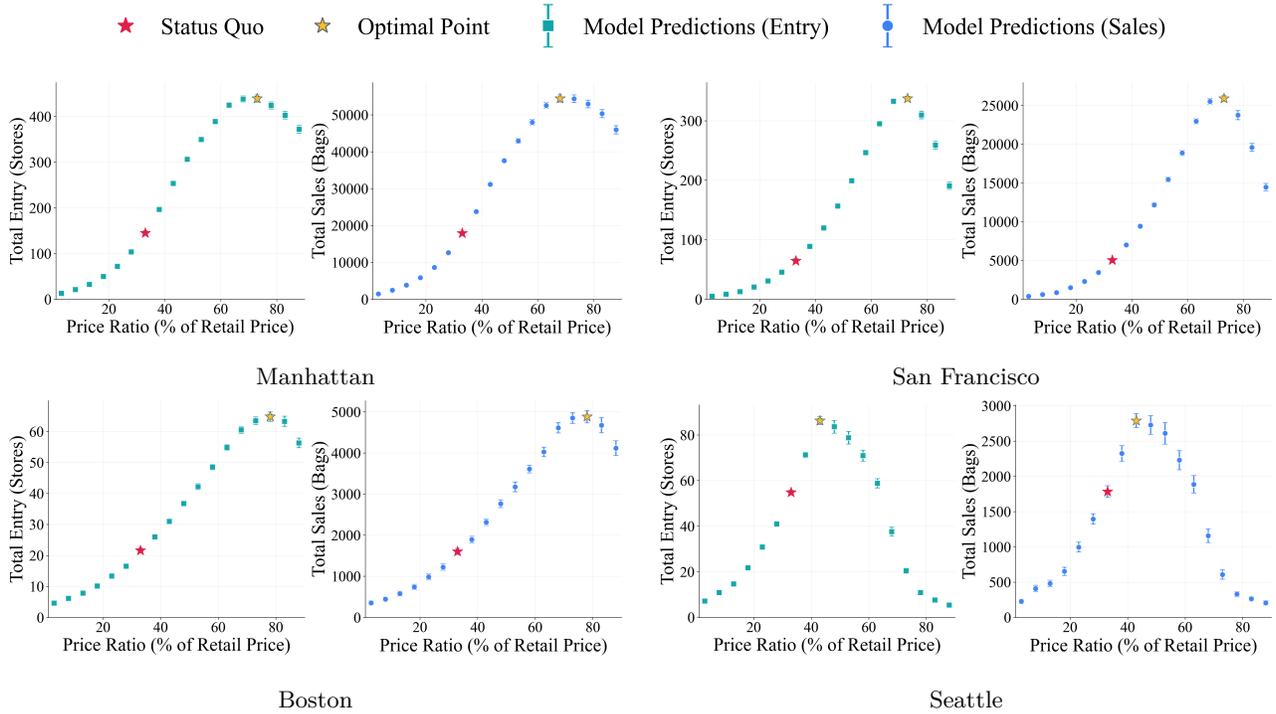
Table 6: Equilibrium Outcomes under Sales-Maximizing Price Ratios.

	Manhattan	San Francisco	Boston	Seattle
Optimal Price Ratio (%)	68.3	73.3	78.3	43.3
Aggregate Sales (thousands)	54.4	25.9	4.88	2.79
Difference in Sales (%)	+204	+414	+205	+56.4
Number of Entrants	438	337	64.8	86.3
Difference in Entrants (%)	+202	+424	+200	+57.4

Notes: Each column reports simulated market outcomes at the optimal uniform price ratio that maximizes aggregate sales. Percentage increases are measured relative to the status-quo price ratio (33% of retail value). Sales are reported in thousands of bags.

Table 6 shows that the optimal price ratio for a sales-maximizing platform is around 70% or higher in most markets, with Seattle being the exception (43%). As shown in Figure 9, the aggregate sales

volume is upward-sloping over a wide range of price ratios, including the current policy of 33%. This suggests that the supply-side of the marketplace is generally more responsive to price changes than demand, and that equilibrium sales volume is primarily dictated by seller entry. This aligns with our observation that inventory is very often binding in the data: Stores sell all of their inventory on the platform on 70–88% of days on average, depending on the market.

These tight supply constraints explain why market outcomes improve dramatically at the optimal price – in Manhattan, Boston and San Francisco, both entry and sales are predicted to triple or quadruple. The outcomes from price optimization are more modest in Seattle by comparison, potentially due to its unique combination of both high seller marginal costs ($14.13/unit) and high consumer travel costs ($2.12/km).

7.2 Should the Platform Allow Seller Price Competition?

Next, we evaluate market outcomes under delegated pricing: A counterfactual in which sellers are profit-maximizing and permitted to set their own price ratios. This requires solving for a price equilibrium among sellers in the marketplace. Conditional on a set of entrants, our approach follows the standard treatment from the literature of Bertrand–Nash price competition under logit-based consumer choice (e.g., Nevo (2001); Dubé et al. (2002)). The full derivation and computational details are provided in Appendix G.

Under delegated pricing, a market equilibrium is defined by a pair $(\boldsymbol{\psi}^*, \mathbf{p}^*(\boldsymbol{\psi}^*))$, which denotes sellers' entry strategies and optimal prices given the set of entrants. For fixed seller strategies $\boldsymbol{\psi}$, the prices $\mathbf{p}^*(\boldsymbol{\psi})$ must satisfy the following condition, which follows from the first-order condition of sellers' profit functions:

$$p_j^*(\boldsymbol{\psi}) = c_j(\boldsymbol{\theta}^c) - \frac{\sum_{\tau \in \mathscr{T}} \lambda_\tau(\boldsymbol{\alpha}) \sum_{\ell \in \mathcal{L}} \sum_{t \in \mathcal{T}} s_{j\ell\tau}^t(\boldsymbol{\psi}; \boldsymbol{\beta})}{\sum_{\tau \in \mathscr{T}} \lambda_\tau(\boldsymbol{\alpha}) \beta_3 \sum_{\ell \in \mathcal{L}} \sum_{t \in \mathcal{T}} s_{j\ell\tau}^t(\boldsymbol{\psi}; \boldsymbol{\beta})(1 - s_{j\ell\tau}^t(\boldsymbol{\psi}; \boldsymbol{\beta}))} \quad \text{for all } j \in \mathcal{J}^+(\boldsymbol{\psi}). \tag{6}$$

Note the expression above is a fixed point condition because each choice probability $s_{j\ell\tau}^t$ depends on a subset of the equilibrium prices $\mathbf{p}^*(\boldsymbol{\psi})$. Because the full equilibrium requires that entry be profitable, a market equilibrium is given by entry decisions and prices $(\boldsymbol{\psi}^*, \mathbf{p}^*(\boldsymbol{\psi}^*))$ that satisfy both (6) and

$$\psi_j^* = \mathbf{1} \left\{ \sum_{\tau \in \mathscr{T}} \left(p_j^*(\boldsymbol{\psi}^*) - c_j(\boldsymbol{\theta}^c) \right) D_{j\tau}(\boldsymbol{\psi}^*; \boldsymbol{\alpha}, \boldsymbol{\beta}) \geq F_m(\boldsymbol{\theta}^F) \right\}. \tag{7}$$

The results are summarized in Table 7. Delegated pricing reduces aggregate sales volume in the marketplace by 58% to 83% compared to the platform's current policy of a uniform price ratio of 33%.

The dramatic contraction in sales is driven by seller exit – the number of participating sellers drops by 35% to 69% depending on the market. These findings suggest that delegating pricing decisions to individual sellers leads to intense price competition in the marketplace, which pushes margins to be negative for a large number of sellers. Figure 10 depicts the distribution of equilibrium prices and marginal costs of entrants under delegated pricing. Average prices increase from \$5–8 per bag to \$8–14, with greater dispersion, with mean marginal costs also increasing conditional on entry.

Table 7: Counterfactual Equilibrium Outcomes Under Price Competition.

	Manhattan	San Francisco	Boston	Seattle
Unit Price ($)				
Uniform	5.7 (0.1)	5.0 (0.1)	4.8 (0.1)	7.7 (0.4)
Delegated	8.4 (0.5)	9.2 (0.7)	13.6 (1.4)	11.2 (1.2)
Difference	+2.8	+4.2	+8.8	+3.5
Number of Entrants				
Uniform	147.4 (11.7)	64.1 (7.9)	20.5 (4.1)	56.2 (6.6)
Delegated	54.4 (5.3)	31.1 (3.2)	13.3 (1.0)	17.7 (1.8)
Difference	−93.0	−33.0	−7.2	−38.5
Aggregate Sales (thousands)				
Uniform	17.50 (1.35)	4.64 (0.60)	1.27 (0.26)	2.36 (0.33)
Delegated	6.61 (0.65)	1.97 (0.24)	0.52 (0.09)	0.41 (0.08)
Difference (%)	−62.2	−57.5	−59.3	−82.5
Aggregate Profit of Entrants (thousands, $)				
Uniform	37.67 (3.95)	8.62 (1.52)	3.48 (1.14)	6.93 (1.25)
Delegated	6.38 (0.52)	1.52 (0.22)	0.15 (0.13)	0.09 (0.13)
Difference (%)	−83.1	−82.3	−95.6	−98.8

Notes: "Uniform" denotes status-quo policy of a 33% price ratio. "Delegated" denotes seller-controlled pricing. For each market, 100 paired simulations were conducted under both pricing mechanisms using identical random seeds, ensuring that each pair shares the same fixed and marginal costs. Standard deviations are reported in parentheses.

These results may appear counterintuitive given that prices and seller participation move in *opposite* directions, in contrast to our predictions under uniform pricing (Section 7.1). The difference is explained by the equilibrium concepts: Here we solve for a Nash equilibrium in both prices and entry, whereas Section 7.1 fixes prices and considers the entry game only. Consequently, with delegated pricing, sellers with strong competitive positions (e.g., high on-platform ratings, desirable locations, and low costs), can credibly threaten aggressive pricing. Anticipating this pressure, weak sellers opt not to enter, instead of competing. The net result is that under delegated pricing, fewer sellers sustain positive margins in equilibrium, allowing them to capture demand at higher prices.

Figure 10: Distributions of Prices and Marginal Costs.
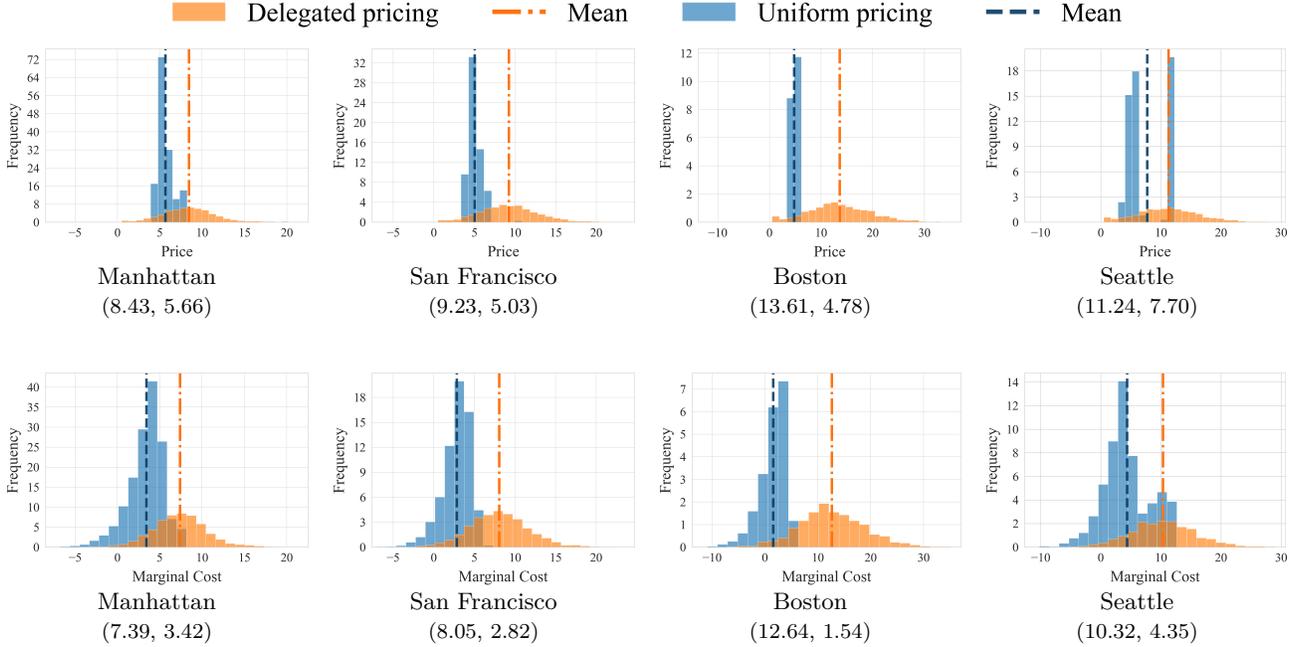
Notes: All plots are based on 100 simulations and share the same legend. In each subfigure, (a, b) denote the mean value of the factor under *delegated pricing* and under *uniform pricing (1/3)*, respectively.

8 Conclusion

This paper addresses the role of pricing as a design lever in surplus food marketplaces. We document three key findings. First, consumer preferences vary substantially across urban environments, influencing competitive dynamics and the performance of different pricing policies. In particular, we find consumers trade-off quality (i.e., sellers' ratings) and convenience (consumer-seller distances) to varying degrees across markets. Second, seller entry is generally more price-elastic than consumer demand, leading supply constraints to bind at most prices. Consequently, steep, market-wide discounts are sub-optimal for the platform. Third, delegating pricing to sellers harms the marketplace: The ensuing price competition slashes margins and prohibits entry, decreasing sales volume by 58–83% compared to the status quo uniform discount rate of two-thirds.

Overall, our findings support centralized control of prices in surplus food marketplaces, which relieves sellers of the excessive competitive pressure associated with seller-controlled pricing. Nonetheless, our results caution platform operators against mandating large discounts on surplus food, which can compress sellers' margins and deter participation in the marketplace.

This paper also contributes methodologically to the literature on empirical models of market entry by introducing an integer optimization–based estimator for sellers' cost functions. In contrast to nested

fixed-point (NFXP) methods, our approach jointly searches over the parameter space and a set of plausible equilibria of the entry game, reducing runtimes by up to an order of magnitude compared to NFXP. Numerical experiments suggest this speed-up does not come at the cost of estimation accuracy, and often improves it. This scalability makes it possible to accommodate richer cost structures with more covariates, providing a new a broadly applicable tool for empirical work on markets with discrete strategic entry.

References

Aguirregabiria, V. and Mira, P. (2007). Sequential estimation of dynamic discrete games. *Econometrica*, 75(1):1–53.

Aguirregabiria, V. and Suzuki, J. (2016). Empirical games of market entry and spatial competition in retail industries. In *Handbook on the Economics of Retailing and Distribution*, pages 201–232. Edward Elgar Publishing.

Akkaş, A. and Gaur, V. (2022). Om forum—reducing food waste: An operations management research agenda. *Manufacturing & Service Operations Management*, 24(3):1261–1275.

Alptekinoglu, A. and Benade, G. (2024). Achieving rawlsian justice in food rescue. *Available at SSRN 4991205*.

Anderson, M. and Magruder, J. (2012). Learning from the crowd: Regression discontinuity estimates of the effects of an online review database. *The Economic Journal*, 122(563):957–989.

Armstrong, M. (2006). Competition in two-sided markets. *The RAND journal of economics*, 37(3):668–691.

Astashkina, E., Belavina, E., and Marinesi, S. (2019). The environmental impact of the advent of online grocery retailing. *Available at SSRN 3358664*.

Astashkina, E., Duenyas, I., and Hu, Y. (2024). Profitability and food waste in buffet restaurants. *Available at SSRN 4993885*.

Bai, B., Chan, T., Zhang, D., Zhang, F., Chen, Y., and Hu, H. (2022a). The value of logistic flexibility in e-commerce. *Available at SSRN 4206229*.

Bai, B., Dai, H., Zhang, D. J., Zhang, F., and Hu, H. (2022b). The impacts of algorithmic work assignment on fairness perceptions and productivity: Evidence from field experiments. *Manufacturing & Service Operations Management*, 24(6):3060–3078.

Bajari, P., Benkard, C. L., and Levin, J. (2007). Estimating dynamic models of imperfect competition. *Econometrica*, 75(5):1331–1370.

Bajari, P., Hong, H., and Ryan, S. P. (2010). Identification and estimation of a discrete game of complete information. *Econometrica*, 78(5):1529–1568.

Belavina, E. (2021). Grocery store density and food waste. *Manufacturing & Service Operations Management*, 23(4):889–904.

Belavina, E., Girotra, K., and Kabra, A. (2017). Online grocery retail: Revenue models and environmental impact. *Management Science*, 63(6):1781–1799.

Berry, S., Levinsohn, J., and Pakes, A. (1995). Automobile prices in market equilibrium. *Econometrica*, 63(4):841–890.

Berry, S. and Reiss, P. (2007). Empirical models of entry and market structure. *Handbook of industrial organization*, 3:1845–1886.

Berry, S. T. (1992). Estimation of a model of entry in the airline industry. *Econometrica: Journal of the Econometric Society*, pages 889–917.

Besbes, O., Fonseca, Y., Lobel, I., and Zheng, F. (2023). Signaling competition in two-sided markets. *Available at SSRN 4451693*.

Bravo, F., Gandhi, A., Hu, J., and Long, E. (2024). Closer to home: A structural estimate-then-optimize approach to improve access to healthcare services. *Management Science*.

Bresnahan, T. F. and Reiss, P. C. (1991). Entry and competition in concentrated markets. *Journal of political economy*, 99(5):977–1009.

Cachon, G. P., Dizdarer, T., and Tsoukalas, G. (2025). Pricing control and regulation on online service platforms. *Management Science*.

Calvo, E., Cui, R., and Wagner, L. (2023). Disclosing product availability in online retail. *Manufacturing & Service Operations Management*, 25(2):427–447.

Cao, X., Zhang, D., and Huang, L. (2022). The impact of the covid-19 pandemic on the behavior of online gig workers. *Manufacturing & Service Operations Management*, 24(5):2611–2628.

Cao, Y., Chevalier, J. A., Handbury, J., Parsley, H., and Williams, K. R. (2024). Distributional impacts of the changing retail landscape. Technical report, Cowles Foundation for Research in Economics, Yale University.

Chevalier, J. A. and Mayzlin, D. (2006). The effect of word of mouth on sales: Online book reviews. *Journal of marketing research*, 43(3):345–354.

Ciliberto, F., Murry, C., and Tamer, E. (2021). Market structure and competition in airline markets. *Journal of Political Economy*, 129(11):2995–3038.

Ciliberto, F. and Tamer, E. (2009). Market structure and multiple equilibria in airline markets. *Econometrica*, 77(6):1791–1828.

Clyde, N., Bai, B., and Zhang, D. (2024). The impact of ridesharing platforms on healthcare access. *Available at SSRN 4968892*.

Collard-Wexler, A. (2013). Demand fluctuations in the ready-mix concrete industry. *Econometrica*, 81(3):1003–1037.

Conlon, C. T. and Mortimer, J. H. (2013). Demand estimation under incomplete product availability. *American Economic Journal: Microeconomics*, 5(4):1–30.

Cragg, J. G. (1971). Some statistical models for limited dependent variables with application to the demand for durable goods. *Econometrica*, 39(5):829–844.

Cui, R., Li, J., and Zhang, D. J. (2020a). Reducing discrimination with reviews in the sharing economy: Evidence from field experiments on airbnb. *Management Science*, 66(3):1071–1094.

Cui, R., Li, M., and Li, Q. (2020b). Value of high-quality logistics: Evidence from a clash between sf express and alibaba. *Management Science*, 66(9):3879–3902.

Cui, R., Lu, Z., Sun, T., and Golden, J. M. (2024). Sooner or later? promising delivery speed in online retail. *Manufacturing & Service Operations Management*, 26(1):233–251.

Cui, R., Zhang, D. J., and Bassamboo, A. (2019). Learning from inventory availability information: Evidence from field experiments on amazon. *Management Science*, 65(3):1216–1235.

Davis, P. (2006). Spatial competition in retail markets: movie theaters. *The RAND Journal of Economics*, 37(4):964–982.

de Almeida Oroski, F. and da Silva, J. M. (2023). Understanding food waste-reducing platforms: A mini-review. *Waste Management & Research*, 41(4):816–827.

den Boer, A. V., Jansen, H. M., and Zhao, J. (2022). Waste reduction of perishable products through markdowns at expiry dates. *Boston University Questrom School of Business Research Paper*, (4151451).

Dubé, J.-P., Chintagunta, P., Petrin, A., Bronnenberg, B., Goettler, R., Seetharaman, P., Sudhir, K., Thomadsen, R., and Zhao, Y. (2002). Structural applications of the discrete choice model. *Marketing letters*, 13:207–220.

Geoffrion, A. M. and Marsten, R. E. (1972). Integer programming algorithms: A framework and state-of-the-art survey. *Management Science*, 18(9):465–491.

Google Maps Platform (2025). Google Places API. https://developers.google.com/maps/documentation/places/web-service/overview. Accessed: 2025-10-16.

Guo, Y., Gao, F., Zhang, W., and Ming, L. (2025). Omnichannel operations in on-demand delivery platform with buy-online-and-pick-up-in-store. *Available at SSRN 4862038*.

Hansen, L. P. (1982). Large sample properties of generalized method of moments estimators. *Econometrica: Journal of the econometric society*, pages 1029–1054.

He, P., Zheng, F., Belavina, E., and Girotra, K. (2021). Customer preference and station network in the london bike-share system. *Management Science*, 67(3):1392–1412.

Hu, Q., Huang, N., and Zhang, R. P. (2024). Viewer traffic allocation for small creator development: Experimental evidence from short-video platforms. *Available at SSRN 4888995*.

Jain, N., Kabra, A., and Karamshetty, V. (2023). Until later is preferred over sooner: Multiplicity in product expiration dates and food waste in retail stores. *Available at SSRN 4317868*.

Jia, P. (2008). What happens when wal-mart comes to town: An empirical analysis of the discount retailing industry. *Econometrica*, 76(6):1263–1316.

Jiang, Z., Li, J., and Zhang, D. (2025). A high-dimensional choice model for online retailing. *Management Science*, 71(4):3320–3339.

Kabra, A., Belavina, E., and Girotra, K. (2020). Bike-share systems: Accessibility and availability. *Management Science*, 66(9):3803–3824.

Kazaz, B., Xu, F., and Yu, H. (2025). Retailing strategies of imperfect produce and the battle against food waste. *Manufacturing & Service Operations Management*.

Lee, K. H. and Musolff, L. (2023). Entry into two-sided markets shaped by platform-guided search. *Princeton University.*

Liu, S., Siddiq, A., and Zhang, J. (2024). Planning bike lanes with data: Ridership, congestion, and path selection. *Management Science.*

Long, X., Sun, J., Dai, H., Zhang, D., Zhang, J., Chen, Y., Hu, H., and Zhao, B. (2024). The choice overload effect in online retailing platforms. *Manufacturing Service Operations Management.*

Lu, Z., Cui, R., Sun, T., and Wu, L. (2023). The value of last-mile delivery in online retail. *Available at SSRN 4590356.*

Makov, T., Shepon, A., Krones, J., Gupta, C., and Chertow, M. (2020). Social and environmental analysis of food waste abatement via the peer-to-peer sharing economy. *Nature communications*, 11(1):1156.

Manshadi, V. and Rodilitz, S. (2020). Online policies for efficient volunteer crowdsourcing. In *Proceedings of the 21st ACM Conference on Economics and Computation*, pages 315–316.

Mazzeo, M. J. (2002). Product choice and oligopoly market structure. *RAND Journal of Economics*, 33(2):221–242.

McFadden, D. (1989). A method of simulated moments for estimation of discrete response models without numerical integration. *Econometrica: Journal of the Econometric Society*, pages 995–1026.

Musalem, A., Olivares, M., Bradlow, E. T., Terwiesch, C., and Corsten, D. (2010). Structural estimation of the effect of out-of-stocks. *Management Science*, 56(7):1180–1197.

Nevo, A. (2001). Measuring market power in the ready-to-eat cereal industry. *Econometrica*, 69(2):307–342.

Pakes, A., Ostrovsky, M., and Berry, S. (2007). Simple estimators for the parameters of discrete dynamic games (with entry/exit examples). *the RAND Journal of Economics*, 38(2):373–399.

Pakes, A. and Pollard, D. (1989). Simulation and the asymptotics of optimization estimators. *Econometrica: Journal of the Econometric Society*, pages 1027–1057.

Park, J.-H., Iancu, D., and Plambeck, E. L. (2022). On the management of premade foods.

Pedregosa, F., Varoquaux, G., Gramfort, A., Michel, V., Thirion, B., Grisel, O., Blondel, M., Prettenhofer, P., Weiss, R., Dubourg, V., et al. (2011). Scikit-learn: Machine learning in python. *Journal of Machine Learning Research*, 12:2825–2830.

Restaurant365 (2023). What is the average restaurant profit margin? Accessed: 2025-05-21.

Richards, T. J. and Hamilton, S. F. (2018). Food waste in the sharing economy. *Food Policy*, 75:109–123.

Rust, J. (1987). Optimal replacement of gmc bus engines: An empirical model of harold zurcher. *Econometrica: Journal of the Econometric Society*, pages 999–1033.

Sanders, R. E. (2024). Dynamic pricing and organic waste bans: A study of grocery retailers' incentives to reduce food waste. *Marketing Science*, 43(2):289–316.

Seim, K. (2006). An empirical model of firm entry with endogenous product-type choices. *The RAND Journal of Economics*, 37(3):619–640.

Stourm, L. and Stourm, V. (2024). Estimating sparse spatial demand to manage crowdsourced supply in the sharing economy. *Marketing Science.*

Su, C.-L. and Judd, K. L. (2012). Constrained optimization approaches to estimation of structural models. *Econometrica*, 80(5):2213–2230.

Thomadsen, R. (2007). Product positioning and competition: The role of location in the fast food industry. *Marketing Science*, 26(6):792–804.

Too Good To Go (2024). 2024 impact report. Technical report, Too Good To Go. Accessed on: 2025-10-14.

Train, K. E. (2009). *Discrete choice methods with simulation*. Cambridge university press.

U.S. Census Bureau (2022). American community survey 5-year estimates.

U.S. Department of Agriculture (2025). Why should we care about food waste? Accessed: 2025-01-29.

Vachon, P. (2025). Grocery stores toss 30% of food: This app lets you buy it for cheap before they do.

Wang, Y., Li, J., and Anupindi, R. (2023). Manufacturing and regulatory barriers to generic drug competition: A structural model approach. *Management Science*, 69(3):1449–1467.

Wolsey, L. A. (2020). *Integer programming*. John Wiley & Sons.

Wolsey, L. A. and Nemhauser, G. L. (1999). *Integer and combinatorial optimization*. John Wiley & Sons.

WRAP (2015). Strategies to achieve economic and environmental gains by reducing food waste. Wrap is an anti-waste organization in Britain. Accessed: 2024-08-26.

Wu, N. and Duarte, V. (2024). This startup brings in $162 million a year helping people find food at huge discounts: It's 'the most genius app'. *CNBC*. Online article.

Yang, L. and Yu, M. (2025). Too good to go: Combating food waste with surprise clearance. *Management Science*.

Yu, N., Belavina, E., and Girotra, K. (2023). Using artificial intelligence to reduce food waste. Technical report, SC Johnson College of Business, Cornell University/Cornell Tech. Available at SSRN: https://ssrn.com/abstract=4826777.

Zeng, Z., Dai, H., Zhang, D. J., Zhang, H., Zhang, R., Xu, Z., and Shen, Z.-J. M. (2023). The impact of social nudges on user-generated content for social network platforms. *Management Science*, 69(9):5189–5208.

Zeng, Z., Zhang, Z., Zhang, D., and Chan, T. (2024). The impact of recommender systems on content consumption and production: Evidence from field experiments and structural modeling. *Available at SSRN*.

Zhang, D. J., Dai, H., Dong, L., Wu, Q., Guo, L., and Liu, X. (2019). The value of pop-up stores on retailing platforms: Evidence from a field experiment with alibaba. *Management Science*, 65(11):5142–5151.

Zhang, W., Zheng, Z., and Cui, R. (2023). Restaurant density and delivery speed in food delivery platforms. *Kelley School of Business Research Paper*, 4419279.

Zhou, F., Astashkina, E., and Anupindi, R. (2024a). Information disclosure in online grocery: Profit and food waste implications. *Available at SSRN 4986854*.

Zhou, F., Jiang, H., Li, A., and Uichanco, J. (2024b). Designing surprise bags for surplus foods. *Available at SSRN*.

Appendix

A   Supplement for Section 2: Data and Marketplace Overview

The screenshots below illustrate the app's interface. The first shows store categories, the second highlights key features like price, rating, pick-up window, and location, and the third reveals the default distance filter (1 mile in Manhattan) which ensures users see only the nearby stores.

Figure 11: Consumer View of Platform App.
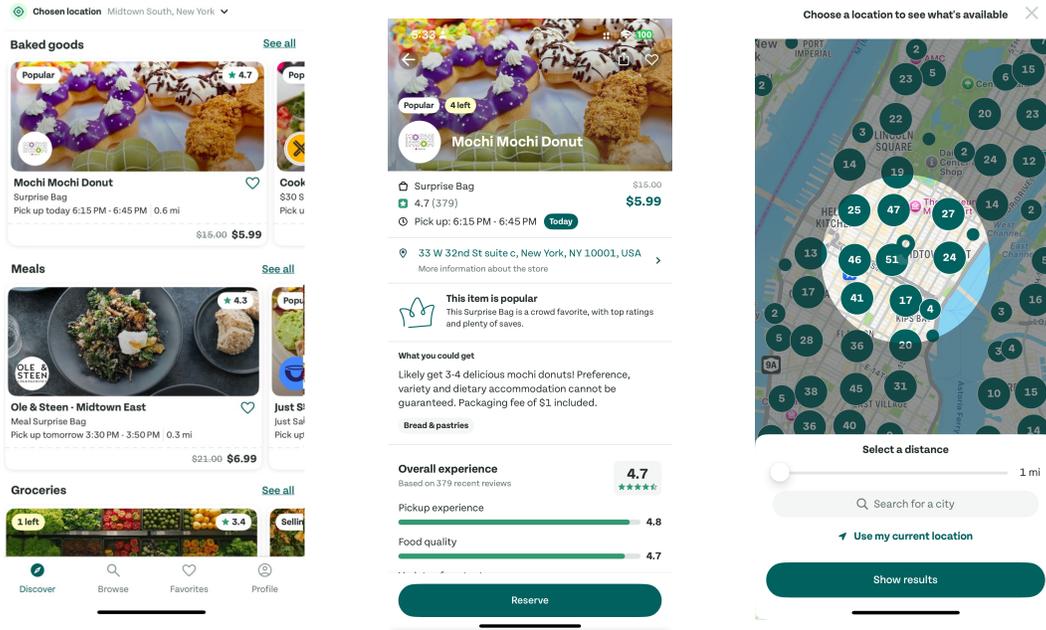
Seller price, rating and location information.

Additional seller details.

Distance-based search filter (1 mile for Manhattan).

Table 8 shows several consecutive rows from the platform data for a specific bakery in New York City. Key features include the store's location, pickup window, inventory levels, sold-out time, platform price, retail price, average rating, and number of ratings.

Table 8: Example of Store-Hour Observations.

Timestamp	Store ID	Store Name	Long.	Lat.	Pickup Start	Pickup End
3/4/24 15:00	384279	Bel Ami Cafe	-73.9670	40.7690	17:00	18:00
3/4/24 16:00	384279	Bel Ami Cafe	-73.9670	40.7690	17:00	18:00
3/4/24 17:00	384279	Bel Ami Cafe	-73.9670	40.7690	17:00	18:00

Items Avail.	Sold Out At	Category	Price	Value	Rating	Rating Count
0	-	BAKED_GOODS	3.99	12.00	4.73	99
3	-	BAKED_GOODS	3.99	12.00	4.73	99
0	16:13	BAKED_GOODS	3.99	12.00	4.73	99

Notes: This example shows that at 15:00, the store had no available stock. By 16:00, three bags were released for pickup between 17:00 and 18:00, and were sold out at 16:13. The bags, with retail value of $12.00, was sold for $3.99.

B Descriptive Statistics

In this section, we present descriptive statistics and visualizations of the study region to aid interpretation of both the data and the estimation results. We begin with an overview of the scale and distribution of bakeries across the four regions, and then report summary statistics for the covariates used in the demand-side and supply-side models.

B.1 Locations of Food Retailers Within Four Geographic Markets

Our inventory data comes from 465 bakeries across the four markets, with locations shown in Figure 12. Manhattan stands out with a much higher retail density (4.81 stores per km^2) compared to the other cities.

Table 9: Summary Statistics of Four Geographic Markets.

	Manhattan	**San Francisco**	**Boston**	**Seattle**
No. Stores	284	94	34	53
No. Census Tracts	270	233	130	137
Area (km^2)	59	120	113	452
Stores per km^2	4.81	0.78	0.30	0.12
Stores per Tract	1.05	0.40	0.26	0.39

B.2 Demand-side Covariates

Table 10 reports the distribution of covariates used in the demand-side model estimation.

Figure 12: Average Daily Sales of Sellers in Four Markets.

Manhattan (284 stores)
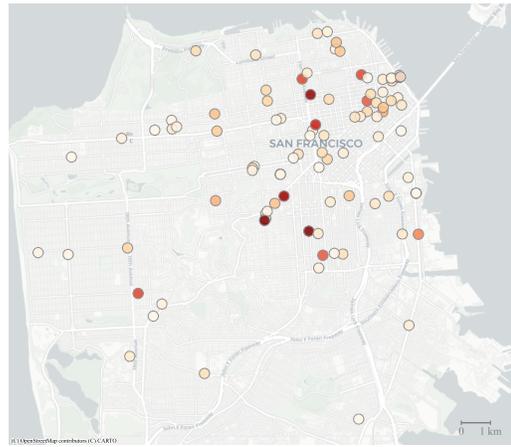
San Francisco (94 stores)
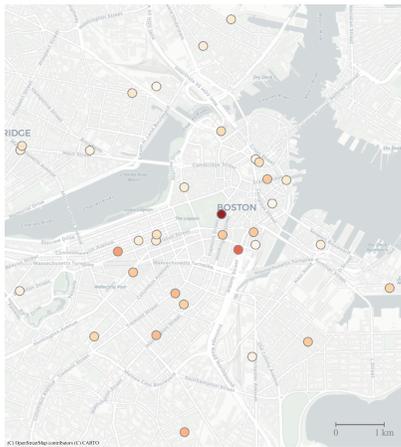
Boston (34 stores)
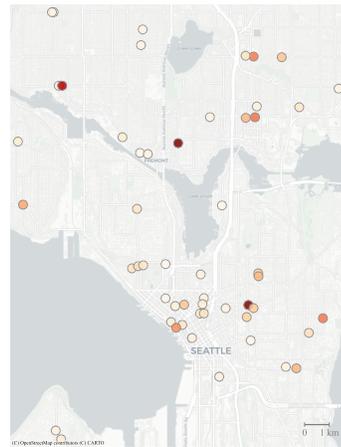
Seattle (53 stores)

Table 10: Summary Statistics of Demand-Model Covariates.

Variable	Manhattan					San Francisco				
	Mean	SD	25%	Median	75%	Mean	SD	25%	Median	75%
PopulationDensity ($/m^2$)	0.037	0.018	0.024	0.037	0.046	0.012	0.009	0.007	0.010	0.014
Weekend	0.17	0.37	0.00	0.00	0.00	0.17	0.37	0.00	0.00	0.00
Income (100k)	1.16	0.60	0.66	1.13	1.60	1.43	0.57	1.03	1.45	1.83
PlatfromRating	4.46	0.31	4.31	4.53	4.68	4.54	0.31	4.44	4.62	4.74
Distance (km)	5.48	3.80	2.49	4.61	7.69	4.97	2.70	2.77	4.63	7.00
BagPrice (USD)	5.42	2.20	3.99	4.99	5.99	4.95	1.20	3.99	4.99	5.99
Discount (USD)	10.86	4.39	8.01	10.01	12.01	9.93	2.39	8.01	10.01	12.01

Variable	Boston					Seattle				
	Mean	SD	25%	Median	75%	Mean	SD	25%	Median	75%
PopulationDensity ($/m^2$)	0.011	0.007	0.007	0.010	0.016	0.007	0.007	0.003	0.005	0.009
Weekend	0.17	0.37	0.00	0.00	0.00	0.17	0.37	0.00	0.00	0.00
Income (100k)	1.03	0.51	0.68	0.94	1.36	1.27	0.47	0.97	1.28	1.56
PlatformRating	4.42	0.27	4.19	4.48	4.66	4.74	0.15	4.67	4.76	4.84
Distance (km)	3.13	1.48	2.02	3.05	4.15	5.47	2.95	3.10	5.30	7.44
BagPrice (USD)	4.79	0.79	3.99	4.99	4.99	5.52	2.17	3.99	4.99	5.99
Discount (USD)	9.61	1.59	8.01	10.01	10.01	11.11	4.45	8.01	10.01	12.01

Notes: PopulationDensity is measured as the number of residents per square meter and calculated at the census-tract level. *Weekend* is an indicator equal to 1 if the observation falls on a weekend and 0 otherwise. *Income* denotes the median household income, expressed in units of $100,000. *PlatformRating* refers to the store's rating on the surplus food marketplace. *Distance* measures the consumer–store distance in kilometers. *BagPrice* is the price paid by consumers for each bag, while *Discount* represents the difference between the primary-market retail value and the discounted price. SD denotes standard deviation.

B.3 Supply-side Covariates

The covariates underlying the entry model estimation are summarized in Table 10.

Table 11: Summary Statistics of Covariates in Sellers' Fixed and Marginal Cost Functions.

Variable	Manhattan					San Francisco				
	Mean	SD	25%	Median	75%	Mean	SD	25%	Median	75%
GoogleRating	4.31	0.41	4.10	4.40	4.60	4.42	0.33	4.20	4.50	4.60
PopulationDensity (k/km^2)	30.9	9.81	21.8	34.2	38.7	9.82	4.68	7.35	8.47	10.6
HoursOpen	73.1	26.8	63.0	76.0	89.8	61.0	26.2	45.5	62.0	77.5
$\log(RatingCount)$	5.26	1.31	4.48	5.46	6.15	5.03	1.21	4.25	5.11	5.89
CoffeeShopIndicator	0.47	0.50	0.00	0.00	1.00	0.29	0.45	0.00	0.00	1.00
StyleIndicator	0.43	0.50	0.00	0.00	1.00	0.56	0.50	0.00	1.00	1.00
MedianHomeValue ($M)	1.32	0.30	1.06	1.35	1.63	1.42	0.21	1.26	1.45	1.60

Variable	Boston					Seattle				
	Mean	SD	25%	Median	75%	Mean	SD	25%	Median	75%
GoogleRating	4.22	0.48	4.10	4.30	4.50	4.45	0.35	4.30	4.50	4.70
PopulationDensity (k/km^2)	12.2	4.71	10.3	13.2	15.2	6.52	4.28	3.94	4.28	6.01
HoursOpen	72.1	25.5	56.0	76.0	89.3	63.1	27.5	46.0	63.0	77.0
$\log(RatingCount)$	5.14	1.24	4.38	5.18	5.89	5.37	1.20	4.60	5.46	6.11
CoffeeShopIndicator	0.42	0.49	0.00	0.00	1.00	0.32	0.47	0.00	0.00	1.00
StyleIndicator	0.34	0.48	0.00	0.00	1.00	0.39	0.49	0.00	0.00	1.00
MedianHomeValue ($M)	0.97	0.25	0.78	0.93	1.04	0.98	0.17	0.90	1.00	1.15

Notes: PopulationDensity is measured as the number of thousands of residents per square kilometer and is calculated at the market-segment (ZIP-code) level. *HoursOpen* denotes the total weekly operating hours of each store, as reported on Google Places. SD denotes standard deviation.

C   Proof of Proposition 1

Without loss of generality, we assume $\mathbb{E}[\bar{p}(R_j)] > c_j$ for all $j \in \mathcal{J}$, otherwise seller j trivially never enters and can be excluded from the entry game. Let $\mathcal{J}_m^+ \subseteq \mathcal{J}_m$ denote an arbitrary set of entrants in segment m. First, Assumption 1 implies seller j's sales depends only on the entry decisions of the other sellers in segment m. Further, Assumption 2 implies that all sellers in the same segment form identical beliefs about their expected sales $\mathbb{E}[S_j]$ and price $\mathbb{E}[\bar{p}(R_j)]$. It follows that the expected sales for each entrant $j \in \mathcal{J}_m^+$ depends only on the total number of entrants $|\mathcal{J}_m^+|$ in the same segment. Thus, we can write each entrant's expected sales as $\mathbb{E}[S_j(|\mathcal{J}_m^+|)]$. Note an entrant $j \in \mathcal{J}_m^+$ has positive profit if and only if $(\mathbb{E}[\bar{p}(R_j)] - c_j) \cdot \mathbb{E}[S_j(|\mathcal{J}_m^+|)] \geq F_m$. Define the threshold function $c_m^*(\cdot) := \mathbb{E}[\bar{p}(R_j)] - F_m/\mathbb{E}[S_j(\cdot)]$. It follows that entrant $j \in \mathcal{J}_m^+$ has positive profit if and only if $c_j \leq c_m^*(|\mathcal{J}_m^+|)$. Next, note $S_j(|\mathcal{J}_m^+|)$ weakly decreases in $|\mathcal{J}_m^+|$ because each additional entrant weakly expands every consumer's choice set, decreasing every seller's demand. It follows that $c_m^*(|\mathcal{J}_m^+|)$ decreases in $|\mathcal{J}_m^+|$. We have thus established that for an arbitrary set of entrants $\mathcal{J}_m^+$, only those with $c_j \leq c_m^*(|\mathcal{J}_m^+|)$ are profitable, and that $c_m^*(|\mathcal{J}_m^+|)$ decreases in $|\mathcal{J}_m^+|$. To identify the unique equilibrium, sort sellers costs in ascending

order $c_{(1)}, c_{(2)}, \ldots, c_{(|J_m|)}$, and let n_m^* be the largest integer such that $c_{(n_m^*)} \leq c^*(n_m^*)$. This integer n_m^* exists and is unique because $c_m^*(n)$ is decreasing in n while $c_{(n)}$ is increasing in n. The unique entry equilibrium for segment m is then given by the set of n_m^* sellers with the smallest marginal costs c_j, with the associated cost threshold given by $c_m^*(n_m^*)$. Note any other configuration would include at least one higher-cost seller who would not be profitable or exclude a lower-cost seller who would find it profitable to enter. $\square$

D   Simulating Seller Market Entry and Sales

In this section we describe the full forward simulation of the estimated model. This is used in the counterfactual analyses and also in evaluating solutions generated by the MMIO estimator.

D.1   Solving Sellers' Entry Game

Here we describe how to compute the equilibrium entry strategy $\boldsymbol{\psi}_m^*$ for each market segment m given model parameters $(\boldsymbol{\alpha}, \boldsymbol{\beta}, \boldsymbol{\zeta}, \boldsymbol{\theta}^c, \boldsymbol{\theta}^F, \sigma^c, \sigma^F)$, which are suppressed hereafter. Under Assumption 2, sellers form profit contribution beliefs by taking expectations over demand $D_{j\tau}$, quantity $Q_{j\tau}$, and bag values V_j. We write $\mathbb{E}[\pi_j(\cdot)]$ to denote these contribution expectations. Next, following Definition 1, for a given market segment m, the strategy profile $\boldsymbol{\psi}_m \subseteq \{0,1\}^{|\mathcal{J}_m|}$ is an equilibrium if and only if

$$\mathbb{E}[\Pi_j(\boldsymbol{\psi}_m)] := \psi_j \cdot [\mathbb{E}[\pi_j(\boldsymbol{\psi}_m)] - F_m] \geq 0 \tag{8}$$

for all $j \in \mathcal{J}_m$, where $\mathbb{E}[\pi_j(\boldsymbol{\psi}_m)]$ is the expected profit contribution before fixed costs. Following Proposition 1, the unique equilibrium entry vector $\boldsymbol{\psi}_m^*$ that solves (8) can be determined by finding a threshold c_m^* such that $\mathbb{E}[\pi_j(\boldsymbol{\psi}_m)] \geq F_m(\boldsymbol{\theta}^F)$ if and only if $c_j \leq c_m^*$. The threshold c_m^* can be determined through a straightforward line search. Algorithm 1 summarizes the steps.

Note that computing the expected sales associated with a set of entrants requires *PlatformRating* and *Price* variables, which are missing data for non-participating retailers. We impute their prices by using the mean price of all active sellers in the retailer's same market segment. To impute *PlatformRating*, we use our sample of participating sellers to estimate a linear regression of *PlatformRating* on the variables *Log(RatingCount)*, *CoffeeShopIndicator*, *StyleIndicator*, and *GoogleRating*, as well as the seller's latitude and longitude. We simulate from the fitted regression model by sampling from the residuals to impute *PlatformRating* for non-participating retailers. The R^2 values vary from 0.08 to 0.13.

ALGORITHM 1: SOLVING SELLERS' ENTRY GAME

Input: Model parameters $(\boldsymbol{\alpha}, \boldsymbol{\beta}, \boldsymbol{\mu}, \boldsymbol{\zeta}, \boldsymbol{\theta}^c, \boldsymbol{\theta}^F)$, simulated cost shocks $(\boldsymbol{\varepsilon}^c, \boldsymbol{\varepsilon}^F)$, segment m.
Output: Equilibrium entry vector $\boldsymbol{\psi}_m^*$.

1. Compute costs $c_j = \theta_0^c + (\boldsymbol{\theta}^c)^\top \mathbf{x}_j + \varepsilon_j^c$ and $F_m = \theta_0^F + (\boldsymbol{\theta}^F)^\top \mathbf{v}_m + \varepsilon_m^F$.
2. Sort sellers by cost: $c_{(1)} \leq c_{(2)} \leq \ldots \leq c_{(|\mathcal{J}_m|)}$.
3. For $n = 1, 2, \ldots, |\mathcal{J}_m|$:
   a. Set $\psi_j = 1$ if $c_j \leq c_{(n)}$ and $\psi_j = 0$ otherwise.
   b. Compute $\mathbb{E}[\pi_j(\boldsymbol{\psi}_m)] \leftarrow \text{EXPECTEDCONTRIBUTION}(\boldsymbol{\psi}_m)$.
   c. If equilibrium condition (8) holds, let $\boldsymbol{\psi}_m^* = \boldsymbol{\psi}_m$, break loop.
4. Return equilibrium entry profile $\boldsymbol{\psi}_m^*$.

Subroutine: EXPECTEDCONTRIBUTION$(\boldsymbol{\psi}_m)$
1. Compute $D_{j\tau} = \sum_{t \in \mathcal{T}} D_{j\tau}^t$ for all $j \in \mathcal{J}_m^+(\boldsymbol{\psi}_m)$ using demand model (2).
2. For $i = 1, 2, \ldots n$ simulations:
   i. For each store $j \in \mathcal{J}_m^+(\boldsymbol{\psi}_m)$ and period $\tau \in \mathscr{T}$ draw inventory $(Q_{j\tau})^i \sim H_j(\mu, \boldsymbol{\zeta})$.
   ii. Compute sales $(S_{j\tau})^i = \min\{D_{j\tau}, (Q_{j\tau})^i\}$.
3. Compute total expected sales

$$\mathbb{E}[S_j] = \frac{1}{|\mathcal{J}_m^+| \cdot n} \sum_{\tau \in \mathscr{T}} \sum_{j' \in \mathcal{J}_m^+} \sum_{i=1}^{n} (S_{j'\tau})^i$$

and expected price

$$\mathbb{E}[p_j] = \frac{1}{|\mathcal{J}_m^+|} \sum_{j' \in \mathcal{J}_m^+} p_{j'}(R_{j'})$$

for $j \in \mathcal{J}_m^+(\boldsymbol{\psi}_m)$.
4. Compute expected contribution $\mathbb{E}[\pi_j(\boldsymbol{\psi}_m)] = (\mathbb{E}[p_j] - c_j) \cdot \mathbb{E}[S_j]$ for $j \in \mathcal{J}_m^+(\boldsymbol{\psi}_m)$.
5. Return $\mathbb{E}[\pi_j(\boldsymbol{\psi}_m)]$ for $j \in \mathcal{J}_m^+(\boldsymbol{\psi}_m)$.

Notes: The exact value of seller j's price $p_j(R_j)$ depends on the pricing policy being simulated. Under uniform pricing, $p_j(R_j) = \bar{p}(R_j)$ (as per Section 3.2); under delegated pricing, $p_j(R_j) = p_j^*(R_j)$ (Section 7.2)

D.2 Simulating Inventory and Sales

Once the entry equilibrium $\boldsymbol{\psi}$ is determined, we simulate total sales for each store by generating individual consumer arrivals and tracking inventory depletion. This is described in Algorithm 2.

ALGORITHM 2: DEMAND AND INVENTORY SIMULATION

Input: Model parameters $(\boldsymbol{\alpha}, \boldsymbol{\beta}, \boldsymbol{\mu}, \boldsymbol{\zeta})$, entry vector $\boldsymbol{\psi}$.
Output: Total sales S_j for each seller $j \in \mathcal{J}$.

---

1. Initialize sales $S_j = 0$ for all $j \in \mathcal{J}$.
2. For each macro-period $\tau \in \mathscr{T}$:
   a. For each $j \in \mathcal{J}$, sample $Q_{j\tau} \sim H_j(\mu, \boldsymbol{\zeta})$. Set starting inventory $Q_{j\tau}^1 = Q_{j\tau}$.
   b. For each granular period $t \in \mathcal{T}$:
      i. Determine available sellers $\mathcal{J}_\tau^t = \{j \in \mathcal{J} : \psi_j = 1 \text{ and } Q_{j\tau}^t > 0\}$.
      ii. Compute demand $D_{j\tau}^t = \sum_{\ell \in \mathcal{L}} \lambda_{\ell\tau}^t \cdot s_{j\ell\tau}^t$ for each $j \in \mathcal{J}_\tau^t$.
      iii. Realize sales $S_{j\tau}^t = \min\{D_{j\tau}^t, Q_{j\tau}^t\}$.
      iv. Update inventory $Q_{j\tau}^{t+1} = Q_{j\tau}^t - S_{j\tau}^t$.
3. Return total sales $S_j = \sum_{t \in \mathcal{T}} \sum_{\tau \in \mathscr{T}} S_{j\tau}^t$ for all $j \in \mathcal{J}$.

E   GMM Estimator for Consumer Arrivals and Choice

E.1   Moment Conditions

We specify three sets of moments for estimation the demand model via GMM. We define $\boldsymbol{\phi} := (\boldsymbol{\alpha}, \boldsymbol{\beta})$ to compactly represent the demand-side parameters. Let $\mathcal{J}$ denote the set of stores, $\mathcal{T}$ the set of time intervals (hours), $\mathscr{T}$ the set of days, $\mathcal{W}$ the set of weeks, and $\mathcal{M}$ the set of market segments. For each store $j \in \mathcal{J}$, hour $t \in \mathcal{T}$, and day $\tau \in \mathscr{T}$, total demand over all locations $\ell \in \mathcal{L}$ is given by:

$$D_{j\tau}^t(\boldsymbol{\phi}, \boldsymbol{\xi}) = \sum_{\ell \in \mathcal{L}} \lambda_{\ell\tau}^t(\boldsymbol{\phi}) \cdot \frac{e^{V_{j\ell}(\boldsymbol{\phi}, \boldsymbol{\xi})} \cdot \mathbf{1}_{\{j \in \mathcal{J}_\tau^t\}}}{1 + \sum_{j' \in \mathcal{J}_\tau^t} e^{V_{j'\ell}(\boldsymbol{\phi}, \boldsymbol{\xi})}}.$$

We define the predicted sales under $(\boldsymbol{\phi}, \boldsymbol{\xi})$ as $\hat{S}_{j\tau}^t(\boldsymbol{\phi}, \boldsymbol{\xi}) := \min\{D_{j\tau}^t(\boldsymbol{\phi}, \boldsymbol{\xi}), Q_{j\tau}^t\}$, where $Q_{j\tau}^t$ represents quantity available. For our first set of moments, we construct store-level sales moments at different levels of temporal aggregation. With a slight abuse of notation, define

$$G_{jt\tau}^1(\boldsymbol{\phi}, \boldsymbol{\xi}) := S_{j\tau}^t - \hat{S}_{j\tau}^t(\boldsymbol{\phi}, \boldsymbol{\xi}) \qquad \text{(store-hourly)}$$

$$G_{j\tau}^1(\boldsymbol{\phi}, \boldsymbol{\xi}) := \sum_{t \in \mathcal{T}} S_{j\tau}^t - \sum_{t \in \mathcal{T}} \hat{S}_{j\tau}^t(\boldsymbol{\phi}, \boldsymbol{\xi}) \qquad \text{(store-daily)}$$

$$G_{jw}^1(\boldsymbol{\phi}, \boldsymbol{\xi}) := \sum_{\tau \in \mathscr{T}_w} \sum_{t \in \mathcal{T}} S_{j\tau}^t - \sum_{\tau \in \mathscr{T}_w} \sum_{t \in \mathcal{T}} \hat{S}_{j\tau}^t(\boldsymbol{\phi}, \boldsymbol{\xi}) \qquad \text{(store-weekly)}$$

$$G_j^1(\boldsymbol{\phi}, \boldsymbol{\xi}) := \sum_{\tau \in \mathscr{T}} \sum_{t \in \mathcal{T}} S_{j\tau}^t - \sum_{\tau \in \mathscr{T}} \sum_{t \in \mathcal{T}} \hat{S}_{j\tau}^t(\boldsymbol{\phi}, \boldsymbol{\xi}) \qquad \text{(store-total)}$$

For our second set of moments, we define segment-level sales by summing over all stores within each segment, specified at the zip code level in particular. Let $\mathcal{J}_m \subset \mathcal{J}$ denote the set of stores in segment $m \in \mathcal{M}$. We construct segment-level moments at different temporal aggregations:

$$G_{mt\tau}^2(\boldsymbol{\phi}, \boldsymbol{\xi}) := \sum_{j \in \mathcal{J}_m} S_{j\tau}^t - \sum_{j \in \mathcal{J}_m} \hat{S}_{j\tau}^t(\boldsymbol{\phi}, \boldsymbol{\xi}) \qquad \text{(segment-hourly)}$$

$$G^2_{m\tau}(\boldsymbol{\phi}, \boldsymbol{\xi}) := \sum_{j \in \mathcal{J}_m} \sum_{t \in \mathcal{T}} S^t_{j\tau} - \sum_{j \in \mathcal{J}_m} \sum_{t \in \mathcal{T}} \hat{S}^t_{j\tau}(\boldsymbol{\phi}, \boldsymbol{\xi}) \qquad \text{(segment-daily)}$$

$$G^2_{mw}(\boldsymbol{\phi}, \boldsymbol{\xi}) := \sum_{j \in \mathcal{J}_m} \sum_{\tau \in \mathcal{T}_w} \sum_{t \in \mathcal{T}} S^t_{j\tau} - \sum_{j \in \mathcal{J}_m} \sum_{\tau \in \mathcal{T}_w} \sum_{t \in \mathcal{T}} \hat{S}^t_{j\tau}(\boldsymbol{\phi}, \boldsymbol{\xi}) \qquad \text{(segment-weekly)}$$

$$G^2_{m}(\boldsymbol{\phi}, \boldsymbol{\xi}) := \sum_{j \in \mathcal{J}_m} \sum_{\tau \in \mathcal{T}} \sum_{t \in \mathcal{T}} S^t_{j\tau} - \sum_{j \in \mathcal{J}_m} \sum_{\tau \in \mathcal{T}} \sum_{t \in \mathcal{T}} \hat{S}^t_{j\tau}(\boldsymbol{\phi}, \boldsymbol{\xi}) \qquad \text{(segment-total)}$$

The third set of moments are the orthogonality conditions that follow from the exclusion criterion assumed to be satisfied by the instruments Z^k_{jm}, $\mathbb{E}\left[Z^k_{jm} \cdot \xi_j\right] = 0$, for each instrument $k \in \{1, 2, \ldots, K\}$. Accordingly, we define

$$G^3_k(\boldsymbol{\xi}) := \sum_{m \in \mathcal{M}} \sum_{j \in \mathcal{J}} Z^k_{jm} \cdot \xi_j \quad \text{(Orthogonality)}$$

We define corresponding sub-vectors:

$$\boldsymbol{\eta}^1(\boldsymbol{\phi}, \boldsymbol{\xi}) := \begin{bmatrix} G^1_{111}(\boldsymbol{\phi}, \boldsymbol{\xi}) \\ \vdots \\ G^1_{|\mathcal{J}||\mathcal{T}||\mathcal{T}|}(\boldsymbol{\phi}, \boldsymbol{\xi}) \\ G^1_{11}(\boldsymbol{\phi}, \boldsymbol{\xi}) \\ \vdots \\ G^1_{|\mathcal{J}||\mathcal{T}|}(\boldsymbol{\phi}, \boldsymbol{\xi}) \\ G^1_{11}(\boldsymbol{\phi}, \boldsymbol{\xi}) \\ \vdots \\ G^1_{|\mathcal{J}||\mathcal{W}|}(\boldsymbol{\phi}, \boldsymbol{\xi}) \\ G^1_1(\boldsymbol{\phi}, \boldsymbol{\xi}) \\ \vdots \\ G^1_{|\mathcal{J}|}(\boldsymbol{\phi}, \boldsymbol{\xi}) \end{bmatrix} \qquad \boldsymbol{\eta}^2(\boldsymbol{\phi}, \boldsymbol{\xi}) := \begin{bmatrix} G^2_{111}(\boldsymbol{\phi}, \boldsymbol{\xi}) \\ \vdots \\ G^2_{|\mathcal{M}||\mathcal{T}||\mathcal{T}|}(\boldsymbol{\phi}, \boldsymbol{\xi}) \\ G^2_{11}(\boldsymbol{\phi}, \boldsymbol{\xi}) \\ \vdots \\ G^2_{|\mathcal{M}||\mathcal{T}|}(\boldsymbol{\phi}, \boldsymbol{\xi}) \\ G^2_{11}(\boldsymbol{\phi}, \boldsymbol{\xi}) \\ \vdots \\ G^2_{|\mathcal{M}||\mathcal{W}|}(\boldsymbol{\phi}, \boldsymbol{\xi}) \\ G^2_1(\boldsymbol{\phi}, \boldsymbol{\xi}) \\ \vdots \\ G^2_{|\mathcal{M}|}(\boldsymbol{\phi}, \boldsymbol{\xi}) \end{bmatrix} \qquad \boldsymbol{\eta}^3(\boldsymbol{\xi}) := \begin{bmatrix} G^3_1(\boldsymbol{\xi}) \\ \vdots \\ G^3_K(\boldsymbol{\xi}) \end{bmatrix}$$

Then the full vector of moments is

$$\boldsymbol{\eta}(\boldsymbol{\phi}, \boldsymbol{\xi}) := \begin{bmatrix} \boldsymbol{\eta}_1(\boldsymbol{\phi}, \boldsymbol{\xi}) \\ \boldsymbol{\eta}_2(\boldsymbol{\phi}, \boldsymbol{\xi}) \\ \boldsymbol{\eta}_3(\boldsymbol{\xi}) \end{bmatrix}$$

We jointly estimate the parameters $(\boldsymbol{\phi}, \boldsymbol{\xi})$ by solving the optimization problem

$$\min_{\boldsymbol{\phi}, \boldsymbol{\xi}} \; \boldsymbol{\eta}(\boldsymbol{\phi}, \boldsymbol{\xi})^\top W \, \boldsymbol{\eta}(\boldsymbol{\phi}, \boldsymbol{\xi}),$$

where W is a positive definite weighting matrix. The GMM estimator was implemented in Python using the `L-BFGS-B` optimizer from the `scipy.optimize` package. To improve convergence and ensure the stability of the estimates, we imposed box constraints on the parameters and supplied an explicit gradient function to the optimizer.

E.2 Instrumental Variables: Locations of Historical Landmarks

In Figure 13, we present the locations of the historical landmarks in Manhattan that are used to construct the instrumental variables for consumer-seller distances. These landmarks are clustered in Lower Manhattan, reflecting the historical concentration of the city center, which coincides with areas of higher store density on the platform. Moreover, these civic buildings were constructed between 1802 and 1933, making them plausibly exogenous to contemporary demand shocks. Their age and institutional function further support this exogeneity, as it is unlikely that individuals would combine a visit to a bakery with a trip to a courthouse. We identify similar civic landmarks to construct instruments for the remaining three US cities.

Concretely, given a set of K historical landmarks, for each seller-consumer pair (j, ℓ) we construct the instrument $Z_{j\ell}^k = |dist(k, \ell) - dist(k, j)|$, where $dist(k, \ell)$ and $dist(j, \ell)$ are the landmark-consumer and landmark-seller Euclidean distances, respectively. The specific form is chosen because we expect landmarks to be located close to commercial locations and further from residential locations, making $Z_{j\ell}^k$ positively correlated with $Distance_{j\ell}$.

We assess the strength of the instruments by estimating a first-stage regression, where $Distance_{j\ell}$ denotes the distance between seller j and consumer location ℓ. The regression includes the proposed instruments as covariates and controls for location fixed effects to account for spatial heterogeneity in baseline distances. Specifically, we estimate

$$Distance_{j\ell} = \eta_0 + \boldsymbol{\eta}^\top \mathbf{Z}_{j\ell} + \delta_\ell + \varepsilon_{j\ell},$$

where $\mathbf{Z}_{j\ell} = (Z_{j\ell}^1, \ldots, Z_{j\ell}^K)^\top$ is the vector of instruments derived from landmark-based distances, $\boldsymbol{\eta}$ is the corresponding coefficient vector, δ_ℓ captures location fixed effects, and $\varepsilon_{j\ell}$ is an idiosyncratic error term. Adding the instruments increases the adjusted R^2 from 0.07 to 0.78, a substantial improvement ($\Delta R^2 = 0.71$) that indicates strong explanatory power for $Distance_{j\ell}$. The joint F-statistic of 3,191 far exceeds the conventional threshold of 10, confirming that the instruments are highly relevant and not weak in the first stage.

Figure 13: Locations of Selected Historical Civic Landmarks in Manhattan.

● Bakery on the platform

(1) Appellate Division of the Supreme Court of the State of New York

(2) Eleventh District Municipal Court

(3) Harlem Courthouse

(4) Jefferson Market Courthouse

(5) Manhattan Third District Magistrate's Courthouse

(6) New York City Hall

(7) New York County Courthouse (New York State Supreme Court)

(8) New York County Courthouse, Tweed Courthouse

(9) Surrogate's Court (Hall of Records)

(10) United States Courthouse

F Estimating Sellers' Entry Costs: Method of Moments with Integer Optimization

This section provides additional details about the integer optimization-based estimation technique for sellers' entry costs discussed in Section 5.3. Section F.3 presents the reformulation of the general moment optimization problem (5). Section F.4 outlines the iterative algorithm based on cutting plane methods for solving the resulting optimization problem. Section F.5 presents numerical comparison between our method and NFXP.

F.1 Generating Candidate Equilibria

We employ a standard implementation of a random forest algorithm to generate candidate equilibria for each market segment. These candidate equilibria represent a set of plausible strategy profiles based on store characteristics and market conditions. For each segment $m \in \mathcal{M}$, the algorithm generates a set of strategy profiles $\{\hat{\boldsymbol{\psi}}_k \in \{0,1\}^{|\mathcal{J}_m|} : k \in \mathcal{K}_m\}$, which are used in the optimization model described below.

To generate these profiles, we train a random forest classifier that predicts store-level entry probabilities using non–TGTG variables as predictors and observed entry as the outcome. The feature set includes store attributes—geographic coordinates, store type, style indicator, Google Map rating rating, and count—obtained or constructed from the Google Places data, along with market segment characteristics, such as median home value, obtained from American Community Survey data. The model is trained using 100 trees with a maximum depth of 10 and balanced class weights, based on an 80/20 train–test split. The resulting test accuracy ranges from 0.81 to 0.93 across the four markets. For each market segment $m \in \mathcal{M}$, we then simulate $|\mathcal{K}_m| = 400$ candidate equilibria by drawing binary vectors of length $|\mathcal{J}_m|$ from independent Bernoulli trials based on the model's predicted entry probabilities, to capture plausible variations in market participation while keeping the computation tractable.

F.2 Variable Construction

Next, we outline how cost covariates in the entry model were constructed from raw data.

MedianHomeValue. Median home values are obtained at the census tract level and aggregated to the ZIP code level. When a ZIP code spans multiple tracts, we take the average of tract-level median home values to construct the ZIP-level measure.

HoursOpen. Operating intensity is measured by total weekly opening hours, $Hours\_Open_j$.

$\log(RatingCount)$. To capture the informativeness of reputation while mitigating skewness, we use $\log(1 + RatingCount_j)$ from the Google Places dataset. Missing values in rating count are imputed as zeros.

StyleIndicator. This variable is constructed from Google Maps' editorial summaries. Each summary is converted into Term Frequency-Inverse Document Frequency (TF–IDF) features that capture key words and short phrases,

implemented via the `TfidfVectorizer` module in `scikit-learn` (Pedregosa et al., 2011). We then apply K-means clustering with two groups, which separates stores with refined descriptions (e.g., "fine dining," "boutique," "exquisite") from those with simpler ones (e.g., "casual," "family-run," "no-frills"), interpreted as upscale (1) and non-upscale (0), respectively. Missing entries are replaced with empty strings and treated as non-upscale.

F.3   Integer Optimization Model Formulation

Let $\psi_j \in \{0,1\}$ be a binary variable where $\psi_j = 1$ if store j enters the market according to the model, and $\psi_j = 0$ otherwise; hence, the vector $\boldsymbol{\psi}$ represents a strategy profile in the entry game. Using the definitions of $\mathbb{E}[\pi_j]$ and F_m, the market entry condition (3) implies the following logical constraints on $\boldsymbol{\psi}$, where we suppress the dependence on $\boldsymbol{\alpha}, \boldsymbol{\beta}, \boldsymbol{\zeta}$ throughout the section:

$$\mathbb{E}[\pi_j(\boldsymbol{\psi}; \boldsymbol{\theta}^c)] - F_m(\boldsymbol{\theta}^F) \leq \bar{\Pi}\psi_j,$$
$$\mathbb{E}[\pi_j(\boldsymbol{\psi}; \boldsymbol{\theta}^c)] - F_m(\boldsymbol{\theta}^F) \geq -\bar{\Pi}(1 - \psi_j).$$

Here, $\bar{\Pi}$ represents a sufficiently large constant equal to the maximum possible profit across all stores. Note that the expected profit depends on both the cost parameters $\boldsymbol{\theta}^F$ and $\boldsymbol{\theta}^c$ and the entry decisions of all stores, $\boldsymbol{\psi}$.

Let $\omega_k \in \{0,1\}$ indicate whether profile $\hat{\boldsymbol{\psi}}_k$ is selected by the optimization model for some $k \in \mathcal{K}_m$. We restrict our attention to the subset of sampled entry strategy profiles by imposing the additional constraints:

$$\psi_j = \sum_{k \in \mathcal{K}_m} \omega_k \hat{\psi}_{jk}, \quad \forall j \in \mathcal{J}_m, \ m \in \mathcal{M},$$

and

$$\sum_{k \in \mathcal{K}_m} \omega_k = 1, \quad \forall m \in \mathcal{M}.$$

Let N_m denote the empirical number of stores entering segment m, and let $\hat{N}_m(\boldsymbol{\theta})$ represent the predicted number of entrants under $\boldsymbol{\theta}$. Given a set of simulated shocks ε_m^F and ε_j^c, we estimate $\boldsymbol{\theta} = (\boldsymbol{\theta}^c, \boldsymbol{\theta}^F)$ by solving the following moment optimization problem:

$$\min_{\boldsymbol{\psi}, \boldsymbol{\theta}, \mathbf{c}, \mathbf{F}} \quad \sum_{m \in \mathcal{M}} |N_m - \hat{N}_m| \tag{9a}$$

$$\text{subject to} \quad (\bar{p}(R_j) - c_j) \sum_{\tau \in \mathscr{T}} \mathbb{E}[\min\{D_{j\tau}(\boldsymbol{\psi}), Q_{j\tau}\}] - F_m \leq \bar{\Pi}\psi_j, \quad \forall j \in \mathcal{J}_m, \ m \in \mathcal{M}, \tag{9b}$$

$$(\bar{p}(R_j) - c_j) \sum_{\tau \in \mathscr{T}} \mathbb{E}[\min\{D_{j\tau}(\boldsymbol{\psi}), Q_{j\tau}\}] - F_m \geq -\bar{\Pi}(1 - \psi_j), \quad \forall j \in \mathcal{J}_m, \ m \in \mathcal{M}, \tag{9c}$$

$$F_m = \theta^F + (\boldsymbol{\theta}^F)^\top \mathbf{v}_m + \varepsilon_m^F, \quad \forall m \in \mathcal{M}, \tag{9d}$$

$$c_j = \theta_0^c + (\boldsymbol{\theta}^c)^\top \mathbf{x}_j + \varepsilon_j^c, \quad \forall j \in \mathcal{J}_m, \ m \in \mathcal{M}, \tag{9e}$$

$$\sum_{j \in \mathcal{J}_m} \psi_j = \hat{N}_m, \quad \forall m \in \mathcal{M}, \tag{9f}$$

$$\psi_j = \sum_{k \in \mathcal{K}_m} \omega_k \hat{\psi}_{jk}, \quad \forall j \in \mathcal{J}_m, \ m \in \mathcal{M}, \tag{9g}$$

$$\sum_{k \in \mathcal{K}_m} \omega_k = 1, \quad \forall m \in \mathcal{M}, \tag{9h}$$

$$\psi_j \in \{0,1\}, \quad \forall j \in \mathcal{J}_m, \ m \in \mathcal{M}, \tag{9i}$$

$$\omega_k \in \{0,1\}, \quad \forall k \in \mathcal{K}_m, \ m \in \mathcal{M}. \tag{9j}$$

Using the exact expression for $\mathbb{E}[\min\{D_{j\tau}(\boldsymbol{\psi}), Q_{j\tau}\}]$ within the optimization problem is intractable for two reasons. First, note $D_{j\tau}$ is the sum of MNL probabilities over $\mathcal{L}$ consumer locations (cf. (2)), which combined with the $\min\{\}$ operator makes computing the expectation complex. Second, the discrete decision variables $\boldsymbol{\psi}$ enter into demand $D_{j\tau}(\boldsymbol{\psi})$ by modifying consumers' choice sets (cf. (1)) within the MNL, which is intractable to optimize over.

We instead take a sample average approximation. First note we have

$$\mathbb{E}[\min\{D_{j\tau}(\boldsymbol{\psi}), Q_{j\tau}\}] = \mathbb{E}\left[\min\left\{D_{j\tau}\left(\sum_{k \in \mathcal{K}_m} \omega_k \hat{\psi}_k\right), Q_{j\tau}\right\}\right] = \sum_{k \in \mathcal{K}_m} \omega_k \mathbb{E}[\min\{D_{j\tau}(\hat{\psi}_k), Q_{j\tau}\}],$$

where the second equality follows from the linearity of expectation and constraints (9g)–(9h). Second, we approximate each term using sample average approximation:

$$\mathbb{E}[\min\{D_{j\tau}(\hat{\psi}_k), Q_{j\tau}\}] \approx \frac{1}{N} \sum_{i=1}^{N} \min\left\{\sum_{\ell \in \mathcal{L}} \lambda_{\ell\tau} \cdot s_{j\ell\tau}(\hat{\psi}_k), Q_{j\tau}^{(i)}\right\},$$

where $Q_{j\tau}^{(i)}$ are independent inventory samples from the estimated hurdle model and $s_{j\ell\tau}(\hat{\psi}_k)$ are pre-computed MNL choice probabilities for candidate profile $\hat{\psi}_k$. Combining the two steps above, we define a new function that is linear in the profile selection variables $\boldsymbol{\omega}$:

$$\rho_{j\tau}(\boldsymbol{\omega}) := \sum_{k \in \mathcal{K}_m} \omega_k \left(\frac{1}{N} \sum_{i=1}^{N} \min\left\{\sum_{\ell \in \mathcal{L}} \lambda_{\ell\tau} \cdot s_{j\ell\tau}(\hat{\psi}_k), Q_{j\tau}^{(i)}\right\}\right) \approx \mathbb{E}[\min\{D_{j\tau}(\boldsymbol{\psi}), Q_{j\tau}\}].$$

Substituting $\rho_{j\tau}(\boldsymbol{\omega})$ into (9b) and (9c) yields a mixed-integer linear program. The resulting estimation problem is significantly more computationally tractable and amenable to cutting plane solution techniques, described next.

F.4 Iterative Generation of Entry Conditions

Here we describe the iterative procedure used to solve the integer optimization problem for estimating sellers' entry costs. The key challenge in solving the original optimization model is the large number of equilibrium conditions (9b) and (9c) that must be enforced simultaneously. Our approach addresses this challenge by focusing only on the most "relevant" equilibrium conditions, which significantly improves computational efficiency while guaranteeing convergence to optimality. The approach is in the spirit of cutting plane methods for large-scale

integer optimization models (Geoffrion and Marsten, 1972; Wolsey and Nemhauser, 1999; Wolsey, 2020).

Conceptually, the solution approach iterates between two steps: First, we construct a master problem where the equilibrium entry conditions (9b) and (9c) are enforced for a small and randomly chosen subset of sellers, which dramatically reduces the number of constraints in the formulation. We then identify in a subproblem sellers whose equilibrium conditions are violated by the incumbent solution, and incorporate those conditions into the master problem. The intuition behind this approach is that focusing exclusively on the constraints that are necessary for finding the optimal solution significantly improves computational efficiency. Importantly, this iterative procedure is guaranteed to terminate at a globally optimal solution of the original problem in a finite number of iterations.[14]

For each segment $m \in \mathcal{M}$, we maintain a subset of sellers $\mathcal{J}_m^+ \subset \mathcal{J}_m$ for whom equilibrium conditions are explicitly enforced. The master problem at iteration k is formulated as

$$\text{MP}^k: \qquad \min_{\boldsymbol{\psi}, \boldsymbol{\theta}, \mathbf{c}, \mathbf{F}} \quad \sum_{m \in \mathcal{M}} |N_m - \hat{N}_m|$$

$$\text{subject to} \quad (\bar{p}(R_j) - c_j(\boldsymbol{\theta})) \sum_{\tau \in \mathcal{T}} \rho_{j\tau}(\boldsymbol{\omega}) - F_m \leq \bar{\Pi}\psi_j, \quad \forall j \in \mathcal{J}_m^+, \ m \in \mathcal{M}, \tag{10a}$$

$$(\bar{p}(R_j) - c_j(\boldsymbol{\theta})) \sum_{\tau \in \mathcal{T}} \rho_{j\tau}(\boldsymbol{\omega}) - F_m \geq -\bar{\Pi}(1 - \psi_j), \quad \forall j \in \mathcal{J}_m^+, \ m \in \mathcal{M}, \tag{10b}$$

$$\text{and } (9d) - (9j).$$

Note that the equilibrium conditions (10a) and (10b) are enforced only for sellers in the subset $\mathcal{J}_m^+$, while all other constraints apply to all sellers. The linearized expected sales function $\rho_{j\tau}(\boldsymbol{\omega})$ is used instead of the original expectation in (9b) and (9c).

After solving the master problem to obtain parameter estimates $\hat{\boldsymbol{\theta}}^k = (\boldsymbol{\theta}^{F,k}, \boldsymbol{\theta}^{c,k})$ and entry decisions $\hat{\boldsymbol{\psi}}^k$ and $\hat{\boldsymbol{\zeta}}^k$, we solve a subproblem for each segment $m \in \mathcal{M}$ to identify sellers with violated equilibrium conditions.

For each segment $m \in \mathcal{M}$, we examine each seller $j \in \mathcal{J}_m \setminus \mathcal{J}_m^+$ and compute a violation measure that quantifies the extent to which the equilibrium entry condition is not satisfied. To keep track of signs correctly, the violation is calculated differently depending on whether the seller enters the market ($\hat{\psi}_j^k = 1$) or not ($\hat{\psi}_j^k = 0$):

$$\Delta_j = \max \left\{ 0, (2\hat{\psi}_j^k - 1) \cdot \left(F_m^k - (\bar{p}(R_j) - c_j^k) \sum_{\tau \in \mathcal{T}} \rho_{j\tau}(\boldsymbol{\zeta}^k) \right) \right\}. \tag{11}$$

We then identify the seller j_m^* with the maximum violation in segment m:

$$j_m^* = \operatorname*{argmax}_{i \in \mathcal{J}_m \setminus \mathcal{J}_m^+} \{\Delta_j\}. \tag{12}$$

If the maximum violation exceeds a pre-specified tolerance $\epsilon > 0$, we add the corresponding seller to the subset: $\mathcal{J}_m^+ \leftarrow \mathcal{J}_m^+ \cup \{j_m^*\}$, and re-solve the master problem. The complete procedure is formalized in Algorithm 3.

---

[14]Convergence to global optimality follows from the fact that there are finitely many potential constraints (i.e., equilibrium conditions) to add, and each iteration either adds at least one condition or terminates with a globally optimal solution.

ALGORITHM 3: METHOD OF MOMENTS WITH INTEGER OPTIMIZATION

Input: Search grid $\Sigma \subset \mathbb{R}_+^2$ for $\boldsymbol{\sigma} = (\sigma^F, \sigma^c)$, number of simulations n, tolerance $\epsilon > 0$, maximum iterations $k_{\max}$.

Output: Parameter estimates $\hat{\boldsymbol{\theta}}$.

Main steps:

1. For each $\boldsymbol{\sigma} \in \Sigma$:

   a. For $i = 1, \ldots, n$ simulations:

      i. Draw cost shocks $(\varepsilon_m^F)^i \sim \mathcal{N}(0, \sigma^F)$ and $(\varepsilon_j^c)^i \sim \mathcal{N}(0, \sigma^c)$ for all $j \in \mathcal{J}_m$, $m \in \mathcal{M}$.

      ii. Obtain estimate $(\tilde{\boldsymbol{\theta}})^i \leftarrow \text{ITERATIVEGENERATION}((\boldsymbol{\varepsilon}^c)^i, (\boldsymbol{\varepsilon}^F)^i)$.

      iii. For each $m \in \mathcal{M}$, compute equilibrium entrants $(\boldsymbol{\psi}_m)^i$ under $(\tilde{\boldsymbol{\theta}})^i$ by solving (8).

      iv. Use ALGORITHM 1 to simulate entry K times under $(\tilde{\boldsymbol{\theta}})^i$. Let Z^i be mean error in entrant count over K simulations.

   b. Let $\tilde{\boldsymbol{\theta}}(\boldsymbol{\sigma}) = \text{argmin}_{\tilde{\boldsymbol{\theta}}^i} Z^i$.

2. Return $\hat{\boldsymbol{\theta}} = \tilde{\boldsymbol{\theta}}(\hat{\boldsymbol{\sigma}})$ where $\hat{\boldsymbol{\sigma}} = \text{argmin}_{\boldsymbol{\sigma} \in \Sigma} \tilde{Z}(\boldsymbol{\sigma})$.

Subroutine: ITERATIVEGENERATION$(\boldsymbol{\varepsilon}^c, \boldsymbol{\varepsilon}^F)$.

1. Initialize $\mathcal{J}_m^+ \subset \mathcal{J}_m$ for each $m \in \mathcal{M}$. Set $k \leftarrow 0$.

2. While $k < k_{\max}$:

   a. Solve master problem MP^k to obtain $(\tilde{\boldsymbol{\theta}})^k$, $(\tilde{\boldsymbol{\psi}})^k$, $(\tilde{\boldsymbol{\zeta}})^k$.

   b. For each $m \in \mathcal{M}$, find j_m^* using (11)–(12). If $\Delta_{j_m^*} > \epsilon$, add j_m^* to $\mathcal{J}_m^+$.

   c. If no violations found, break and return $\tilde{\boldsymbol{\theta}} = (\tilde{\boldsymbol{\theta}})^k$; otherwise set $k \leftarrow k + 1$.

In summary, at each iteration, the algorithm first solves the master problem to obtain current parameter estimates and entry decisions. It then identifies, for each segment, the seller with the most severely violated equilibrium condition. If any violations above the tolerance level ϵ are found, these sellers are added to the subsets $\mathcal{J}_m^+$, and the process continues. The algorithm terminates when either no violations are found or the maximum number of iterations is reached. This approach enhances computational efficiency by focusing exclusively on the constraints necessary for finding the optimal solution, rather than enforcing all equilibrium conditions simultaneously. A summary is given in Algorithm 3.

F.5 Numerical Comparison with Nested Fixed Point Estimation

We compare the performance of our proposed method with a straightforward implementation of NFXP using synthetic data. To evaluate scalability, we consider two setups: one that increases the geographic scope of the market (e.g., more zip code regions), and another that increases model complexity by adding more cost covariates. Results are presented in Table 12 and visualized in Figure 14.

In Setup 1, we fix the number of cost covariates and vary the number of market segments, where each segment has 20–80 randomly generated stores. Except for the case with only two segments — where the estimate for $\boldsymbol{\theta}^F$ is less accurate — the proposed method consistently outperforms NFXP, achieving lower RMSE and RRMSE with significantly shorter runtimes, particularly as market size increases. In Setup 2, we fix the number of market segments and vary the number of marginal cost covariates. Again, except for the case with only one

covariates, the proposed method delivers more accurate estimates than NFXP while requiring less than one-tenth the computation time. Both setups highlight the accuracy and scalability of our approach.


ALGORITHM 4: NESTED FIXED POINT ESTIMATION FOR SELLERS' COST PARAMETERS

Input: Parameter grid $\Theta = \{(\boldsymbol{\theta}_1^c, \boldsymbol{\theta}_1^F), \ldots, (\boldsymbol{\theta}_K^c, \boldsymbol{\theta}_K^F)\}$, empirical entry counts $\{N_m\}_{m \in \mathcal{M}}$.
Output: Parameter estimates $\hat{\boldsymbol{\theta}} = (\hat{\boldsymbol{\theta}}^c, \hat{\boldsymbol{\theta}}^F)$.

---

1. Initialize best objective $O^* \leftarrow \infty$ and estimate $\hat{\boldsymbol{\theta}} \leftarrow \emptyset$.
2. For each $i = 1, 2, \ldots, n$, draw shocks $(\varepsilon_m^F)^i \sim \mathcal{N}(0, \sigma^F)$ and $(\varepsilon_j^c)^i \sim \mathcal{N}(0, \sigma^c)$ for $j \in \mathcal{J}_m$, $m \in \mathcal{M}$.
3. For each candidate parameter $(\boldsymbol{\theta}^c, \boldsymbol{\theta}^F) \in \Theta$:
   a. For each segment $m \in \mathcal{M}$ and $i = 1, 2, \ldots, n$, solve entry game with ALGORITHM 1 to obtain equilibrium strategies $\{(\boldsymbol{\psi}_m^*)^i\}_{i=1}^n$.
   b. Set predicted entrants $(\hat{N}_m)^i \leftarrow \sum_{j \in \mathcal{J}_m} (\psi_j^*)^i$ for all $i = 1, 2, \ldots, n$.
   c. Compute current objective $O \leftarrow \sum_{r=1}^R \sum_{m \in \mathcal{M}} |N_m - (\hat{N}_m)^i|$.
   d. If $O < O^*$, update $\hat{\boldsymbol{\theta}} \leftarrow (\boldsymbol{\theta}^c, \boldsymbol{\theta}^F)$ and $O^* \leftarrow O$.
4. Return $\hat{\boldsymbol{\theta}}$.

Figure 14: Observed vs. Predicted Entrants on Synthetic Instances.
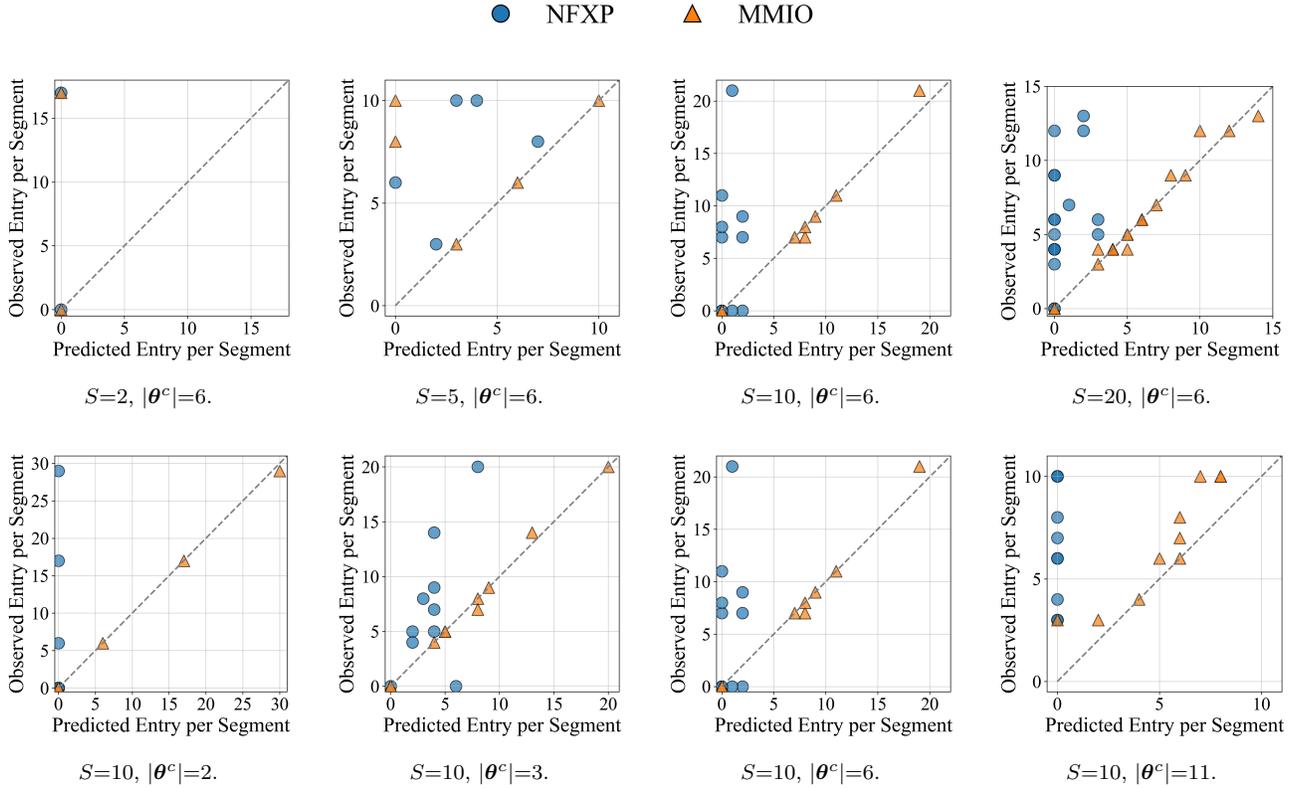
Notes: S represents the number of market segments, and $|\boldsymbol{\theta}^c|$ denotes the number of coefficients estimated for the marginal cost covariates, including the intercept. All instances are for 2 fixed cost parameters ($|\boldsymbol{\theta}^F| = 2$).

Table 12: Performance of MMIO and NFXP Estimators on Synthetic Instances.

Setup 1: Varying Number of Segments

Number of Segments	$|\boldsymbol{\theta}^c|$	$|\boldsymbol{\theta}^F|$	Number of Stores	Entry Ratio	Runtime (min)	RMSE $(\boldsymbol{\theta}^c)$	RMSE $(\boldsymbol{\theta}^F)$	RRMSE $(\boldsymbol{\theta}^c)$	RRMSE $(\boldsymbol{\theta}^F)$	Mean Objective Value
MMIO										
2	6	2	120	0.14	3	1.00	183.62	0.33	1.65	1.13
5	6	2	247	0.15	7	0.33	17.47	0.06	0.21	0.00
10	6	2	476	0.13	89	0.29	16.63	0.10	0.16	1.94
20	6	2	971	0.12	73	0.83	12.31	0.23	0.68	0.00
NFXP										
2	6	2	120	0.14	156	1.51	54.53	0.50	0.49	178.20
5	6	2	247	0.15	497	1.43	34.35	0.26	0.42	44.60
10	6	2	476	0.13	1342	1.23	46.78	0.42	0.46	231.20
20	6	2	971	0.12	1519	1.56	16.78	0.43	0.93	288.38

Setup 2: Varying Number of Parameters

Number of Segments	$|\boldsymbol{\theta}^c|$	$|\boldsymbol{\theta}^F|$	Number of Stores	Entry Ratio	Runtime (min)	RMSE $(\boldsymbol{\theta}^c)$	RMSE $(\boldsymbol{\theta}^F)$	RRMSE $(\boldsymbol{\theta}^c)$	RRMSE $(\boldsymbol{\theta}^F)$	Mean Objective Value
MMIO										
10	2	2	449	0.12	6	1.74	17.91	0.42	0.31	0.15
10	3	2	476	0.15	46	0.75	15.27	0.18	0.21	0.28
10	6	2	476	0.13	89	0.29	16.63	0.10	0.16	1.94
10	11	2	449	0.15	86	0.31	22.36	0.08	0.64	0.43
NFXP										
10	2	2	449	0.12	610	0.75	14.73	0.18	0.26	624.00
10	3	2	476	0.15	1189	2.16	40.56	0.52	0.55	219.40
10	6	2	476	0.13	1342	1.23	46.78	0.42	0.46	231.20
10	11	2	449	0.15	1202	1.41	24.18	0.37	0.69	324.60

Notes: (1) $|\boldsymbol{\theta}^c|$ is the number of coefficients to be estimated for the marginal cost covariates, including the intercept; $|\boldsymbol{\theta}^F|$ is for the fixed cost.
(2) RMSE: Root Mean Square Error.
(3) RRMSE: Relative Root Mean Square Error to normalize for the magnitude of the coefficients. (4) Results are based on a fixed $(\sigma^c, \sigma^F) = (0.05, 0.05)$.

G Simulating Market Equilibrium Under Price Competition

In section 7.2, we consider a counterfactual where sellers can choose their own prices. Here we derive the corresponding equilibrium pricing conditions. We assume sellers compete according to Bertrand-Nash pricing and derive the price equilibrium accordingly, which follows closely from standard treatments in the literature (e.g., Nevo (2001); Dubé et al. (2002)). This setup assumes that stores ignore their inventory constraints when setting prices, which is necessarily to preserve tractability of the pricing game. The procedure iterates between solving the store-level pricing first-order conditions under the MNL demand system and updating the set of entrants based on profitability. The full procedure is outlined in Algorithm 4.

First, fix the seller strategies $\boldsymbol{\psi}$ and consider the partial equilibrium in price. Let $\mathcal{J}^+(\boldsymbol{\psi}) := \{j \in \mathcal{J} | \psi_j = 1\}$ be the corresponding set of entrants, and let $\mathcal{J}_\tau^t(\boldsymbol{\psi}) \subseteq \mathcal{J}^+(\boldsymbol{\psi})$ be the set of entrants with available inventory at (t, τ). Under the MNL specification, the estimated probability that a consumer at location ℓ chooses seller j at time (t, τ) is

$$s_{j\ell\tau}^t(\boldsymbol{\psi}; \boldsymbol{\beta}) = \frac{e^{V_{j\ell}(\boldsymbol{\beta})}}{1 + \displaystyle\sum_{j' \in \mathcal{J}_\tau^t(\boldsymbol{\psi})} e^{V_{j'\ell}(\boldsymbol{\beta})}} \cdot \mathbf{1}_{\{j \in \mathcal{J}_\tau^t(\boldsymbol{\psi}) \cup \{0\}\}}$$

where $V_{j\ell}(\boldsymbol{\beta})$ is the estimated deterministic component of utility. The aggregate estimated demand for the entrant $j \in \mathcal{J}^+(\boldsymbol{\psi})$ in period τ is given by

$$D_{j\tau}(\boldsymbol{\psi}; \boldsymbol{\alpha}, \boldsymbol{\beta}) = \lambda_\tau(\boldsymbol{\alpha}) \sum_{\ell \in \mathcal{L}} \sum_{t \in \mathcal{T}} s_{j\ell\tau}^t(\boldsymbol{\psi}; \boldsymbol{\beta}).$$

where $\lambda_\tau(\boldsymbol{\alpha})$ denotes the total market size for period τ. Summing over τ, the expected profit for seller j is

$$\sum_{\tau \in \mathcal{T}} (p_j - c_j(\boldsymbol{\theta}^c)) D_{j\tau}(\boldsymbol{\psi}; \boldsymbol{\alpha}, \boldsymbol{\beta}),$$

where $c_j(\boldsymbol{\theta}^c)$ denotes the marginal cost as a function of the estimated cost parameters. Each entrant sets its bag price p_j to maximize its aggregate expected profit over all periods τ. Treating the bag price p_j as the decision variable, the first-order condition for seller j's profit maximization problem with respect to p_j is

$$\frac{\partial}{\partial p_j} \sum_{\tau \in \mathcal{T}} (p_j - c_j(\boldsymbol{\theta}^c)) D_{j\tau}(\boldsymbol{\psi}; \boldsymbol{\alpha}, \boldsymbol{\beta}) = \sum_{\tau \in \mathcal{T}} \left[D_{j\tau}(\boldsymbol{\psi}; \boldsymbol{\alpha}, \boldsymbol{\beta}) + (p_j - c_j(\boldsymbol{\theta}^c)) \frac{\partial D_{j\tau}(\boldsymbol{\psi}; \boldsymbol{\alpha}, \boldsymbol{\beta})}{\partial p_j} \right] = 0.$$

Momentarily suppressing notation and rearranging, the optimal pricing rule for seller j is characterized by

$$p_j = c_j - \frac{\displaystyle\sum_{\tau \in \mathcal{T}} D_{j\tau}}{\displaystyle\sum_{\tau \in \mathcal{T}} \frac{\partial D_{j\tau}}{\partial p_j}}.$$

Using the expression for $D_{j\tau}$ above, its derivative with respect to p_j is

$$\frac{\partial D_{j\tau}}{\partial p_j} = \lambda_\tau \sum_{\ell \in \mathcal{L}} \sum_{t \in \mathcal{T}} \frac{\partial s_{j\ell\tau}^t}{\partial p_j}.$$

Because only the term $\beta_3 p_j$ in $V_{j\ell}$ depends on p_j, from the MNL probabilities above we have

$$\frac{\partial s^t_{j\ell\tau}}{\partial p_j} = \beta_3 s^t_{j\ell\tau}(1 - s^t_{j\ell\tau}).$$

Thus, for fixed seller strategies $\boldsymbol{\psi}$, the market's (partial) equilibrium prices $\mathbf{p}^*(\boldsymbol{\psi})$ must satisfy

$$p_j^*(\boldsymbol{\psi}) = c_j(\boldsymbol{\theta}^c) - \frac{\displaystyle\sum_{\tau \in \mathscr{T}} \lambda_\tau(\boldsymbol{\alpha}) \sum_{\ell \in \mathcal{L}} \sum_{t \in \mathcal{T}} s^t_{j\ell\tau}(\boldsymbol{\psi}; \boldsymbol{\beta})}{\displaystyle\sum_{\tau \in \mathscr{T}} \lambda_\tau(\boldsymbol{\alpha}) \beta_3 \sum_{\ell \in \mathcal{L}} \sum_{t \in \mathcal{T}} s^t_{j\ell\tau}(\boldsymbol{\psi}; \boldsymbol{\beta})(1 - s^t_{j\ell\tau}(\boldsymbol{\psi}; \boldsymbol{\beta}))} \quad \text{for all } j \in \mathcal{J}^+(\boldsymbol{\psi}). \tag{13}$$

Note the expression above describes a fixed point condition because each choice probability $s^t_{j\ell\tau}$ depends on a subset of the equilibrium prices $\mathbf{p}^*(\boldsymbol{\psi})$. Finally, because the full equilibrium requires that entry be profitable, a market equilibrium is given by entry decisions and prices $(\boldsymbol{\psi}^*, \mathbf{p}^*(\boldsymbol{\psi}^*))$ that satisfy

$$\psi_j^* = \mathbf{1}\left\{ \sum_{\tau \in \mathscr{T}} \left(p_j^*(\boldsymbol{\psi}^*) - c_j(\boldsymbol{\theta}^c) \right) D_{j\tau}(\boldsymbol{\psi}^*; \boldsymbol{\alpha}, \boldsymbol{\beta}) \geq F_m(\boldsymbol{\theta}^F) \right\}, \quad \text{for all } j \in \mathcal{J}_m, \ m \in \mathcal{M}. \tag{14}$$

We use the following iterative procedure to compute a market equilibrium. Starting with an initial candidate set of entrants, we compute the price equilibrium using a damped fixed–point iteration on the first-order conditions (13). This is further refined by a Newton solve of the system (13) (Powell–hybrid via `scipy.optimize.root`). Convergence is declared once the mean absolute residual falls below a tolerance ε_p. Given these prices, we then update the set of entrants by identifying the sellers for whom entry is profitable under the incumbent prices and entrants. The process is repeated until no further changes occur in the set of entrants, which implies satisfaction of (14). Intuitively, the algorithm converges because entry typically reduces incumbents' profits while exit increases the remaining sellers' profits, eventually reaching a stable set of entrants (and associated prices) that constitutes the market equilibrium. Algorithm 5 formalizes the procedure. In practice, the pricing equilibrium and entry conditions are solved to within small tolerances to improve numerical stability.

ALGORITHM 5: SIMULATING MARKET EQUILIBRIUM UNDER PRICE COMPETITION

Input: Model parameters $(\boldsymbol{\alpha}, \boldsymbol{\beta}, \boldsymbol{\mu}, \boldsymbol{\zeta}, \boldsymbol{\theta}^c, \boldsymbol{\theta}^F, \sigma^c, \sigma^F)$, number of simulations n.
Output: Simulated entry counts $\{(N_m)^i\}_{i=1}^n$ for all $m \in \mathcal{M}$ and sales $\{(S_j)^i\}_{i=1}^n$ for all $j \in \mathcal{J}$.

---

1. For $i = 1, 2, \ldots, n$:
    a. Draw cost shocks $(\varepsilon_m^F)^i \sim \mathcal{N}(0, \sigma^F)$ and $(\varepsilon_j^c)^i \sim \mathcal{N}(0, \sigma^c)$, and compute $(c_j)^i$ and $(F_m)^i$ for all $j \in \mathcal{J}_m, \ m \in \mathcal{M}$.
        i. Set $k \leftarrow 0$. Initialize $\boldsymbol{\psi}^k$ to a vector of ones.
        ii. Solve (13) under $\boldsymbol{\psi}^k$ and obtain prices $\mathbf{p}^*(\boldsymbol{\psi}^k)$.
        iii. Compute all seller profits: $\tilde{\Pi}_j = \sum_{\tau \in \mathscr{T}} \left(p_j^*(\boldsymbol{\psi}^k) - (c_j)^i \right) D_{j\tau}\left(\boldsymbol{\psi}^k \right) - (F_m)^i$.
        iv. Set $\psi_j^{k+1} = \mathbf{1}\{\tilde{\Pi}_j \geq 0\}$ for all $j \in \mathcal{J}$. If $\boldsymbol{\psi}^{k+1} = \boldsymbol{\psi}^k$, let $(\boldsymbol{\psi}^*)^i = \boldsymbol{\psi}^k$ and break loop, otherwise update $k \leftarrow k + 1$ and return to Step ii.
    b. Simulate sales $(S_j)^i$ under $(\boldsymbol{\psi}^*)^i$ for each store $j \in \mathcal{J}$ using Algorithm 2.
2. Return simulated entry counts $\{(N_m)^i = \sum_{j \in \mathcal{J}_m}(\psi_j^*)^i\}_{i=1}^n$ for all $m \in \mathcal{M}$ and sales $\{(S_j)^i\}_{i=1}^n$ for all $j \in \mathcal{J}$.